A Lungfish survivor of the end-Devonian extinction and an Early Carboniferous dipnoan radiation.

Tom J. Challands[1*], Timothy R. Smithson,[2] Jennifer A. Clack[2], Carys E. Bennett[3], John E. A. Marshall[4], Sarah M. Wallace-Johnson[5], Henrietta Hill[2]

[1]School of Geosciences, University of Edinburgh, Grant Institute, James Hutton Road, Edinburgh, EH9 3FE, UK. email: tom.challands@ed.ac.uk; tel: +44 (0) 131 650 4849

[2]University Museum of Zoology Cambridge, Downing Street, Cambridge CB2 3EJ, UK.

[3]Department of Geology, University of Leicester, Leicester LE1 7RH, UK.

[4]School of Ocean & Earth Science, University of Southampton, National Oceanography Centre, European Way, University Road, Southampton, SO14 3ZH , UK.

[5]Sedgwick Museum, Department of Earth Sciences, University of Cambridge, Downing St., Cambridge CB2 3EQ, UK

Abstract

Until recently the immediate aftermath of the Hangenberg event of the Famennian Stage (Upper Devonian) was considered to have decimated sarcopterygian groups, including lungfish, with only two taxa, *Occludus romeri* and *Sagenodus* spp., being unequivocally recorded from rocks of Tournaisian age (Mississippian, Early Carboniferous). Recent discoveries of numerous morphologically diverse lungfish tooth plates from southern Scotland and northern England indicate that at least ten dipnoan taxa existed during the earliest Carboniferous. Of these taxa, only two, *Xylognathus* and *Ballgadus*, preserve cranial and post-cranial skeletal elements that are yet to be described. Here we present a description of the skull of a new genus and species of lungfish, *Limanichthys fraseri* gen. et sp. nov. that hails from the very earliest Tournaisian in the Ballagan Formation of Burnmouth, southern Scotland. The new specimen represents the earliest definitive Tournaisian lungfish skull material thus providing an invaluable insight into the response of this group, and indeed, the Sarcopterygii as a whole, immediately following the latest Devonian Hangenberg event. Phylogenetic analysis places *Limanichthys fraseri* within the Devonian 'phaneropleurid-fleurantiid' grade of lungfish and that the Carboniferous lungfish represent forms that have their origins deep in the Mid and Late Devonian as well as those from a unique Carboniferous radiation.

Key words: Dipnoi, Tournaisian, lungfish, Hangenberg, Ballagan Formation, Carboniferous

Introduction

The Tournaisian Stage of the Early Carboniferous (Mississippian) has recently been considered as a period of time possessing a characteristic recovery fauna following the end-Devonian extinction event (Smithson *et al.* 2015). During the Famennian-Tournaisian (the Devonian-Carboniferous boundary) diversity and abundance of sarcopterygian fish at the genus level declined abruptly as chondrichthyans and actinopterygians diversified rapidly in the early Tournaisian (Sallan & Coates 2010; Friedman & Sallan 2012). Additionally, the individuals within the groups are considered to have become smaller during the transition from the Late Devonian to Early Carboniferous, a possible result of nutrient deprivation in the aftermath of the Hangenberg extinction event (Sallan & Galimberti 2015). Though by no means diverse compared to the Middle and Upper Devonian, recent discoveries have shown that lungfishes were not as greatly affected by this episode as previously thought with total dipnoan taxa being more or less constant from the Famennian through to the Tournaisian (Smithson *et al.* 2015).

Several remarkable differences are noticeable between Late Devonian lungfishes and Early Carboniferous lungfish: Carboniferous forms are almost exclusively found in non-marine environments whereas Devonian lungfish occupied both freshwater and marine environments; wide (length to width ratio <1), ‘spoon-shaped’ tooth plates with parallel to sub-parallel ridges, typified by the genus *Ctenodus*, appear for the first time; a dichotomy in size between tooth plates occurs with very small and very large tooth plates being present (Smithson *et al*. 2015) and, all currently known Carboniferous lungfishes possess cartilaginous or poorly-ossified neurocrania. The reduction of ossified cranial tissue has been hypothesised to be due to paedomorphosis and/or change in water chemistrythe environmental conditions of the time (Bemis 1984; Pardo *et al.* 2014) whereby reduction of skull ossification is the most energetically efficient means of development in on a global scale . The lower Tournaisian marks a period of recovery from the Upper Devonian

Hangenberg crisis which saw a complex sequence of glacioeustatic sea-level change and associated carbon burial and reworking represented by a pronounced double carbon isotope spike (Kaiser *et al*. 2016). Further to the loss of a bony neurocranium, all Carboniferous lungfishes possess an unossified or poorly ossified rostrum though the extent of this is variable and less extreme than in post-Carboniferous lungfishes (Kemp *et al.* 2017).

The loss of or poor ossification of the neurocranium and rostrum in Carboniferous lungfish is by no means unique to this time. Several Devonian forms ranging from the Mid Devonian (*Pentlandia*) to the Late Devonian (*Howidipterus*, *Barwickia*, *Rhynchodipterus*, *Soederberghia*, *Phaneropleuron*, *Scaumenacia*, *Nielsenia* and *Jarvikia*) also possessed either a poorly-ossified or unossified neurocranium and/or rostrum (Lehman 1959; Long 1992; Cloutier 1997; Friedman 2007a; Challands & Den Blauuwen 2016). Such observations imply that Carboniferous lungfishes were not innovative in terms of skull construction but whether loss of ossification is homoplastic or not has not been readily investigated. To do so would require a thorough assessment of the phylogenetic relationships and character evolution between Devonian lungfishes and the all Carboniferous lungfish taxa which, to date, has not been completed. However, previously Schultze & Chorn (1997) compiled a character matrix of eighteen taxa from the Devonian to Recent while Lloyd *et al*. (2012) included nine Carboniferous taxa in their analysis of evolutionary rates of the Dipnoi from the Devonian to Recent. The only monophyletic group in Carboniferous lungfish that Lloyd *et al*. (2012) recognised comprised *Tranodis* as the sister taxon to *Straitonia* and *Occludus romeri* (formerly *Ctenodus romeri* Thomson 1965). *Gnathorhiza* was recognised as the most derived of the Carboniferous lungfishes whereas *Delatitia* as the most primitive, the latter forming a clade with the ‘phaneropleurid-fleurantiids’ *Pentlandia*, *Scaumenacia* and *Howidipterus*. The range of *Delatitia* is confined to the Early Carboniferous and its association with the ‘phaneropleurids-fleurantiids’ implies a deep root to this taxon in the Devonian. We address herein the possibility of a

similar Devonian origin for other Carboniferous taxa, specifically the new taxon we describe, and argue

that the Tournaisian Stage did not represent a characteristic recovery fauna for the lungfishes but a time of diversification of a new clade alongside those with a more ancient lineage.

Materials and methods

Specimen NMS G 2017.10.2 was collected in 2014 from the foreshore at Burnmouth, 5 miles (8 km) north of Berwick upon Tweed, in the Scottish Borders. It was found in a black sandy siltstone, 34.5 metres above the base of the Ballagan Formation, in rocks exposed at very low tides outside the harbour wall, and recovered using conventional excavation techniques (hammer and chisel). Following extraction the block containing the specimen was cut to size using a diamond-tipped lapping saw. The part was microCT scanned at the University of Cambridge, Department of Zoology using an X-Tek microCT Scanner producing a voxel resolution of 12 µm. The resulting 1439 scan slices (see supplemental data) were pre-processed in Fiji (Schindelin *et al*. 2012) automatically adjusting for brightness and contrast and partially correcting for beam hardening using the *subtract background* process in Fiji. Segmentation of the skeletal elements was conducted in Materialize Mimics v. 17.0. Photographs of the specimen were taken using a Nikon D5200 digital SLR using

Phylogenetic analysis

Rather than undertaking an exclusive analysis of Devonian or Carboniferous taxa, our aim here is to derive hypotheses of relationships between taxa from both Periods so that the phylogenetic signal from as broad a suite of taxa as possible influences the overall phylogeny. Such an approach comes at the cost of including some taxa with few known character states and so we expect low support for some clades. However, we consider such a direction to be more prefereable than that of a

reductionist approach whereby characters are constructed and used specifically to tease apart the relationships of a small cohort of contemporary taxa (by Period). Such a reductionist approach is, in essence, an *a posteriori* statement that the investigator expects there to be a coherent phylogeny for the taxa chosen.

Bayesian phylogenetic analysis was conducted in MrBayes v. 3.2.6. using a GTR model with a gamma distribution. Four runs were conducted independently each with two chains for 10000000 generations, a sampling frequency of 1000 and a burn-in fraction of 25%. Characters 3, 40, 61, 72, 107 and 138 were ordered.

Parsimony analysis was performed using T.N.T. software (Goloboff *et al*. 2008) following the procedure outlined in Clack *et al* (2016). A total of 100 000 trees were selected as the maximum size of tree space for the exploration of alternative tree topologies. Initial trees were calculated using a New Technology search with ratchet and drift options implemented. We chose 10 replicates (random stepwise addition sequences of taxa), keeping a maximum of five trees at the end of each replicate, using the bisection–reconnection algorithm for tree branch swapping and retaining all trees found at the end of all replicates. A new round of branch swapping was then applied to all trees retained from the initial search (‘trees from RAM’ box ticked). For each set of experiments, where applicable, we summarized the results in the form of a strict consensus . Characters 3, 40, 61, 72, 107 & 138 were ordered.

Our character matrix requires a dataset that describes the morphological variation of both Devonian and post-Devonian taxa and so to achieve this we have used the matrix of Clack *et al*. (2018). This dataset comprises characters used by Challands & Den Blaauwen (2016) as well as those (where not duplicated) from Lloyd *et al*. (2012), the former concerning Devonian taxa exclusively, the latter Devonian-Recent taxa. The most recent character matrix concerning Carboniferous and post-Palaeozoic lungfish from Kemp *et al*. (2017) was designed to elucidate relationships between Carboniferous lungfish and more recent taxa. It produces a lack of resolution

between Devonian taxa with many Devonian taxa scoring '0' for all characters. Additionally, we have recoded fifteen characters from the Kemp *et al*. (2017) matrix and rerun their analysis using the parameters given above (see supplemental data). In addition to the matrix of Clack *et al*. (2018) we have included the post-Carboniferous taxon *Persephonichthys*. Taxa that are only known from mandibles and tooth plates, including *Chirodipterus rhenanus*, *Sunwapta* and *Holodipterus santacrucensis*, were omitted from the analysis.

Characters used in the matrix

Integration of multiple character schemes runs the risk of duplication of characters. While this has been avoided where possible, it is recognised that no definitive scheme is applicable that has been specifically designed for the Dipnoi as a whole. Defining such a character scheme is a matter of much urgency because not all the characters used herein are comprehensively defined. For instance, characters 167 and 175 (characters 22 and 37 of Schultze & Marshall 1993, respectively) are essentially different permutations of describing the arrangement of the dermal bones and so contain overlap. That said, we employ the characters used in the recent analysis of Clack *et al.* (2018) in order to make our analysis comparable with well-established previous hypotheses that use subsections of the characters we have used. Those characters that are clear repetitions have been removed and are highlighted in the supplemental information of Clack *et al*. (2018).

Geological setting

The skull material described herein originated from the Ballagan Formation of Burnmouth, Scotland (Fig. 1), from the VI palynozone, dated as 348–346.6 Ma (Smithson *et al*. 2012, Marshall *et al*. in press). The fossils occur within a sandy siltstone bed near to the base of the formation, at British National Grid Reference NT 395800, 661000, 34.5 m above the base of the Ballagan Formation which approximates to the Devonian-Carboniferous boundary. The bed is a black sandy

siltstone comprising matrix-supported siltstone with millimetre sized clasts of grey, green or black siltstone. The thickness of the bed varies laterally (15-30 cm thick) as does the internal structure (structureless to weakly bedded). This unit contains the oldest tetrapod material of the Ballagan Formation, with associated indeterminate bones (Clack *et al*. 2016). Other fossils within the bed are gyracanthid spines, *Ageleodus* teeth, rhizodont and actinopterygian scales, ostracods, plant and charcoal fragments. The sandy siltstone facies has been identified as the most vertebrate fossil-rich units in the Ballagan Formation (Bennett *et al*. 2016).

The Ballagan Formation comprises ten facies and three facies associations, each of which occur throughout the formation; 1) fluvial facies association; 2) overbank facies association; and 3) saline-hypersaline lake facies association (Bennett *et al*. 2016). The sandy siltstone facies occurs within the overbank facies association, and are interpreted to have formed as cohesive flows resulting from seasonal flood events, picking up sediment clasts and fossil material from desiccated floodplain lakes and vegetated ground as the flood travelled (Bennett *et al*. 2016). The beds either deposited material into depressions on a dry vegetated floodplain, or into existing floodplain lakes or pools. The dipnoan-bearing bed occurs above a series of three 5-10 cm thick very fine sandstone beds, which are rooted but otherwise unmodified indicative of entisol palaeosols (Kearsey *et al*. 2016). Overlying these sandstones is a 10 cm thick laminated grey siltstone. The contact between the fossil-bearing bed and the underlying siltstone is obscured by poor exposure. The environment of deposition is interpreted to have been within a temporary lake on the floodplain.

Results

Several schemes have been used in the past for description of the skull roof bones of lungfish (Forster-Cooper 1937; Jarvik 1967). Of these, the one that has been adopted the most is that of Forster-Cooper (1937) and it is this terminology that is adopted herein.

The anatomical terminology and measurements made for tooth plates follow those used by Smithson *et al*. (2015).

Specimen description

Superclass **Osteichthyes** Huxley, 1880

Class **Sarcopterygii** Romer, 1955

unranked **Dipnomorpha** Ahlberg, 1991

Subclass **Dipnoi** Müller, 1845

Family **undesignated**

Genus ***Limanichthys*** gen. nov.

(Figs 2, 3, 4, 5, 6, 7)

LSID http://zoobank.org/urn:lsid:zoobank.org:act:0EC0B9D2-0672-45A2-900D-44D93A6DC12F

Type species. *Limanichthys fraseri sp. nov.*

Diagnosis. Dipnoan with unossified neurocranium in which anterolateral margin of the Y_1-bone contacts the posterolateral margin of the X-bone and the posterior margin of the X-bone contacts the anterior margin of the I-bone. Paired C-bones that contact two thirds of the length of the medial margin of the fused K-L-bones.

Derivation of name. From the Greek λιμάνι Limani, harbour, and ιχθύς Ichthys, fish, referring to the discovery of the type specimen in the beds outside the harbour at Burnmouth.

Limanichthys fraseri sp. nov.

LSID http://zoobank.org/urn:lsid:zoobank.org:act:0EC0B9D2-0672-45A2-900D-44D93A6DC12F

Derivation of name. From the Latin form of Fraser in honour of Nicholas Fraser, Keeper of Natural Sciences, National Museums Scotland who retrieved and collected the specimen.

Type material. NMS G 2017.10.2a,b

Material. NMS G 2017.10.2a (part) and NMS G 2017.10.2 b (counterpart). UMZC 2017.5.10a, b, c; a large block of black sandy siltstone, sawn into three pieces, containing an operculum and other disarticulated skull bones, a tooth plate with a single row of teeth, and a number of ribs.

Type locality and horizon. Black sandy siltstone *c.* 33 m above the base of the Ballagan Formation on the foreshore at Burnmouth, 20 m north of the outer harbour wall, Scottish Borders, Scotland.

Description. The type specimen comprises a part and counterpart of a slightly disarticulated skull roof and palate with the lateral dorsal skull bones having moved anteromedially over the medial skull bones such that the K-L, J- and I-bones appear to lie more anteriorly than expected (Fig. 2). This gives the impression of two layers of bone. The counterpart (NMS G 2017.10.2 b) contains the parasphenoid and approximately half of the skull roof material revealing the visceral surface of the skull roof bones. The parasphenoid lies dorsal to the skull roof having been moved post mortem. Several scales are present on the counterpart and a large gyracanthid spine has also come to lie on top of the skull roof.

The B-bone is 63 mm long and has an imperfectly preserved posterior margin. The anterior margin possesses an anteromedian process inserting into the midline between the C-bones. An

inverted 'V' depression/ridge in the centre of the visceral surface of the B-bone indicates the position of the median crista while the dorsal surface reveals several fine radiating ridges from the centre of the bone. No lateral line canals or pores are observed in the exposed anterodorsal portion of the B-bone. While the state of preservation precludes the presence of anterolateral processes on the B-bone, and the width of the B-bone cannot be measured accurately because the lateral margins are broken, the maximum width is estimated to be 39 mm based on the impression of the lost bone and the margin with the adjacent I-bone. The lateral margin of the B-bone contacts the medial margin of the I-bone.

The C-bones are almost completely preserved and are hexagonal in shape with margins of unequal length and a distinctive anterior process that projects forward to lie lateral to the D-bone. The anterior-most portion of this process meets the posterior margin of the E-bones. Sitting between the anterior processes of the C-bones is a large, single hexagonal D-bone. The C-bones are 65 mm long by 28 mm wide whereas the D-bone is 32 mm long by 15 mm wide. At the centre of the D-bone, the visceral surface bears a single circular indentation, possibly a vestigial indication of a pineal foramen but the depression does not appear to penetrate through the D-bone. Whether such a circular structure is present on the dermal surface of the D-bone cannot be ascertained.

Like *Ctenodus* (Sharp & Clack 2013, fig. 27) the anterior portion of the I-bone possesses an anterolateral process that contacts the posterior margin of the X-bone or X-Y_1 bone and the medial margins of the Y_1 and Y_2 bones (Fig. 3 D). The anteromedial margin of the I-bone is longer, is concave in shape and contacts the posterolateral margin of the J-bone. A large posterior process, similar to that seen in *Ctenodus* is present (seen most clearly in the counterpart NMS G 2017.10.2 b, Fig. 2 B, D) and extends beyond the posterior margin of the B-bone. A series of lateral line grooves descending into pores are present in the dorsal face of the I-bone traversing from the anterolateral margin next to the Y_2-bone to the medial margin. The pores can be seen to bifurcate and radiate from a central point. It is not clear whether the lateral line pores continue medially into the B-bone.

Anteromedially to the I-bones lie the J-bones which are elongate with a rounded posterolateral margin. Their shape differs from the J-bones of *Ctenodus* which are shorter and has a more angular posterolateral margin and are more similar to *Uronemus* (Watson & Gill 1923). However, unlike the J-bones of *Uronemus* the lateral margin contacts the X-bone alone rather than a fused X-Y_1-bone (Fig. 3 A, F). The medial contact of the J-bone with the C-bone also differs from *Uronemus* and *Ctenodus* in being more than 50% the length of the J-bone.

The most anterior of the lateral series of skull roof bones is a combined K-L-bone which possesses an anteromedial margin contacting the E-bone for approximately one third of its length while the other two thirds contact the C-bone. The lateral line groove seen in the X-bone does not traverse the posterolateral margin of the K-L-bone and no evidence of lateral line pores or grooves are seen in this bone. A fused K-L bone is a variable character with some taxa being polymorphic possessing either a fused K-L-bone or separate K- and L-bones (e.g. *Pentlandia*, Challands & Den Blaauwen 2016, fig. 2 c; *Chirodipterus australis*, Miles 1977, fig. 118 d; and *Amadeodipterus*, Young & Schultze 2005, fig 4 b). The condition of a fused K-L bone is known in other pre-Carboniferous taxa including *Jarvikia* (Lehman 1959, fig. 22), *Oervegia* (Lehman 1959), *Phaneropleuron* (Traquair 1871) possibly *Rhinodipterus kimberleyensis* (Clement 2012) and *Rhinodipterus ulrichi* (Ørvig 1961).

The lateral line is represented not by a series of distinct pores as in, for instance, *Dipterus* (White 1965), but by a series of radial grooves descending into pores that converge towards the centre of the bone. These grooves and pores forming the lateral line canal system are carried anteroposteriorly by the X, Y_1, Y_2-bones and medially by the I-bone. The lateral line bifurcates in the X-bone with one branch directed laterally into bone 4 of the cheek which is not preserved in the specimen.

The X-bone is shaped similarly to the combined X-Y-bone of *Uronemus* (Watson & Gill 1923; Westoll 1949) and *Ctenodus allodens* as figured by Sharp & Clack (2013; fig. 9) though is

distinguished as being a single bone in this case by having a single ossification centre. An incomplete and broken Z-bone is also visible posterior to the Y_2-bone but it is not possible to discern the course of the lateral line canal through it. Whereas the lateral line may bifurcate in bone 4, sending a branch into circumorbital bone 3 (the supraorbital lateral line), bone 4 seldom contacts the Y_1-bone. In *Ctenodus* where bone 4 *does* contact the Y_1-bone, it does not possess a bifurcation of the lateral line canal and, furthermore, bone 4 does not contact the J-bone. This rules out misidentification of the X-bone as bone 4 in specimen NMS G 2017.10.2 despite it having similar morphology to bone 4 in *Uronemus* and *Ctenodus allodens*.

The E-bones are of approximately equal in length to the B- and C-bones and expand laterally towards their anterior such that the anterior margin is twice as wide as the posterior margin. *Ctenodus* differs from *Limanichthys* in possessing E-bones having a medial margin much shorter (approximately 50%) than the lateral margin. Together, this arrangement forms a deep v-shaped notch in the anterior margin of the paired E-bones that, in *Ctenodus*, *Conchopoma* and *Uronemus*, houses the F-bone. This v-shaped notch is shallow in *Limanichthys* and no F-bone is preserved.

The parasphenoid is incompletely preserved with the majority of the corpus missing. From the preservation of the impression of the posterior portion of the corpus the expansion of the corpus from the stalk is smooth and very wide and estimated to be more than twice the width of the stalk at its widest point (Fig. 4 A-C). The parasphenoid stalk in *Limanichthys* is long, posteriorly expanding, strongly ridged, and curves medially at the posterior end to a single fine point. The stalk lies level with the corpus of the parasphenoid.

The operculum in UMZC 2017.5.10b (Fig. 5) is preserved in external view. It is slightly concealed by an overlying gyracanthid spine. The bone is subcircular in outline, with a maximum diameter of 110 mm. It was crushed flat postmortem and bears many cracks across its surface suggesting the operculum was outwardly convex in life. It is finely pitted, but lacks obvious

ornament. The position of the damaged tabulate process on the anterior edge of the bone indicates the specimen is from the right.

An incomplete cranial rib is preserved on UMZC 2017.5.10c (Fig. 5). Judging by the specimen attributed to *Sagenodus copeanus* (Schulze & Chorn 1997 fig. 37), only the distal part of the bone is present. The proximal end and an area overlying a lower jaw element had been eroded away prior to collection. The intact rib was probably *c.* 70 mm long. It appears to have been hollow originally but was crushed flat postmortem. It is 14 mm broad at the distal end and tapers to less than half this width proximally.

Dentition. No palatal dentition is preserved in specimen NMS G 2017.10.2 but microCT scanning of the part (NMS G 2017.10.2a) reveals a single marginal dental element in close proximity to and lying dorsal to the parasphenoid. The element is 4 mm long and possesses seven simple cusps that become smaller posteriorly (Fig. 6). Such a pattern of dentition superficially resembles that seen in the lateral vomerine teeth of *Andreyevichthys* (Krupina & Reisz, 1999) though the resolution of the scan precludes confident assignation to this type of element. Dermopalatine dentitions (e.g. in *Persephonichthys*, Pardo *et al*. 2014) and even vestigial dentaries (e.g. *Pentlandia*, Challands 2015) bear a similar morphology.

A much larger dental element, *c.*15 mm long, is preserved on UMZC 2017.5.10c. It is a single tooth ridge bearing seven teeth (Figs 5, 7). The first six teeth are fused together, the seventh and largest is separate. The tips of all the teeth are worn exposing the mix of dark and light dentine seen in the worn teeth on typical lungfish tooth plates. The teeth are cone-shaped and become progressively larger along the row. The diameter of the first tooth is ~1.3 mm, that of the last is ~2.5 mm. There is no evidence that this toothed element is a broken fragment of a larger tooth plate, but instead it too looks similar to the vomerine tooth plates figured in Krupina & Reisz (1999, fig. 1 c). Similar single tooth ridges have been found in slightly younger rocks in the Ballagan Formation at

Willie's Hole. These may belong to *Ctenodus williei* (Smithson *et al*. 2015) and will be described in due course. The occurrence of palatal tooth plates in Early Carboniferous lungfish adds to the growing evidence (Challands *et al*. 2016, Smithson *et al*. 2015) that following the end-Devonian extinction event the dipnoan dentition was more varied than previously recognised (Smithson *et al*. in press).

Phylogenetic analysis

The present analysis is the most complete analysis of all Devonian and Carboniferous lungfish in the light of the recent discoveries of taxa from the Tournaisian of the United Kingdom. The resulting parsimony analysis produces 27 most parsimonius trees (MPTs) of length 883 (CI = 0.29, RI = 0.61) and a well-resolved strict consensus tree (length = 898, CI = 0.28, RI = 0.60) for all lungfish except for small polytomies containing *Scaumenacia* and *Delatitia*, *Rhinodipterus*, *Phaneropleuron* and a new taxon from Greenland, *Celsiodon* (Clack *et al*. 2018), and for the early-diverging lungfishes *Archaeonectes*, *Chirodipterus onawayensis*, *Chirodipterus wildungensis* and *Dipnorhynchus cathlesae*. (Fig. 8). Node support (Bremer decay indices) for clades are low throughout. Bayesian analysis produced a poorly resolved 50% compatibility tree (Fig. 9) but if all posterior probabilities for branches are used, including those <50% the Bayesian analysis produces a tree topology largely similar to that of the parsimony analysis but with differences in placement of key taxa (branches with posterior probability <50%, see supplementary information).

In the Bayesian analysis *Limanichthys* resolves as sister taxon to *Pentlandia* with posterior probability of 58%. This clade falls out more basal to all other Carboniferous lungfish in the parsimony analysis towards the base of what has been called the phaneropleurid-fleurantiid grade (Challands & Den Blauuwen, 2016). The parsimony result is consistent with previous analyses (Schultze & Chorn, 1997; Lloyd *et al* 2011) in which *Delatitia* resolves as the most basal Carboniferous lungfish, but whereas Schultze & Chorn (1997) resolve *Delatitia* at the base of *all*

other Carboniferous forms, Lloyd *et al.* (2011) resolve *Delatitia* among the phaneropleurid-fleurantiid grade as the current analyses do. The more derived position of *Ctenodus* with *Straitonia* in the Bayesian analysis is in contrast with the parsimony analysis and previous analyses (Schultze & Chorn, 1997; Lloyd *et al*., 2011; Challands & Den Blauuwen, 2016; Clack *et al*. 2018). The parsimony analysis places *Phaneropleuron* towards the base of the phaneropleurid-fleurantiid grade and *Harajicadipterus* and *Orlovichthys* are relegated to a more basal position relative to *Phaneropleuron*. The Bayesian solution does not resolve *Phaneropleuron.*

The strict consensus tree of the parsimony analysis also places *Limanichthys* as the sister taxon to the Givetian form *Pentlandia*. *Phaneropleuron*, the three species of *Rhinodipterus* plus a new taxon described from Greenland, *Celsiodon*, (Clack *et al*, 2018) form a poylotomy basal to Limanichthys + Pentlandia and this is likely attributed to the unstable position of the poorly described *Phaneropleuron. Limanichthys* and *Pentlandia* are supported by a single character reversal (character 53 - posterior parasphenoid stalk converges). It is worth noting that the derived state of character 155 (poorly ossified or cartilagenous neurocranium) is shared by *Phaneropleuron* and all taxa above as well as being independently derived in *Rhynchodipterus* and *Soederberghia* Whereas *Phaneropleuron* resolves in a position consistent with earlier analyses (Friedman 2007b), previous analysis of the phaneropleurid-fleurantiid grade by Challands & Den Blauuwen (2016) failed to place *Phaneropleuron* within this group. The present analysis still does not unequivocally place *Phaneropleuron* within the phaneropleurid-fleurantiid grade, but this inconsistency appears to be partly resolved with the present new dataset which places *Phaneropleuron* in this grade in 18 of the 27 most parsimonious trees.

All Carboniferous taxa (exluding *Limanichthys*, *Delatitia* but also including *Persephonichthys*) form a monophyletic clade in the parsimony analysis defined by two characters (characters 52 and 143) of which the former is a reversal. The Carboniferous dipnoan clade in the Bayesian analysis contains the same taxa in different groupings, however, unlike the previous

analysis Clack *et al*. (2018), *Nielsenia* is unresolved but in the parsimony analysis it resolves with the phaneropleurid-fleurantiids. A Carboniferous lungfish clade is supported by a low posterior probability (57%) and support is also low for groupings higher in the tree including the clade containing *Tranodis* + (*Ctenodus* + *Straitonia*) (61%) and the most derived clade comprising *Conchopoma* + *Parasagenodus* (*Gnathorhiza* +(*Palaeophichthys* + *Persephonichthys*) (72%). The grouping in this most derived clade is consistent between Bayesian and parsimony analyses. The clade forming the *Gnathorhiza* + (*Palaeophichthys* + Persephonichthys) clade is defined by seven characters (characters 19, 37, 45, 170, 175, 177 and 185) with a Bremer decay index of 2. Characters 37 and 45 are reversals while characters 170, 175, 177 and 185 are ambiguous. The posterior probability supporting this clade is low at 57%.

Discussion

Comparison with other dipnoans

There are currently eighteen Carboniferous dipnoan genera known, eleven of which are represented by skull material. Superficially, *Limanichthys* most closely resembles *Ctenodus* but differs in several key morphological characteristics. *Ctenodus murchisoni* as figured in Sharp & Clack (2013) (fig. 10 a, NHMUK P 5031) has a fused X-Y_1-bone which, incidentally, is labelled as the Y_2-bone, the conventional numbering of the Y-bones being reversed (the Y_1-bone is typically anterior to the Y_2-bone). In specimen NMS G 2017.10.2 the Y_2-bone is small and located posterolaterally to the Y_1-bone but the X-bone and Y_1-bone are clearly separate. *Ctenodus interruptus*, *Ctenodus cristatus* and *Uronemus* also possess a fused X- and Y_1-bone. *Ctenodus allodens*, the only species of *Ctenodus* that possesses separate X- and Y_1-bones, can be clearly differentiated from *Limanichthys* in having an X-bone that does not contact the J-bone. This difference in *Ctenodus allodens* from all other species of *Ctenodus* may indicate an incorrect generic assignation. Discriminating *Limanichthys* on the basis of the formal diagnosis of *Ctenodus allodens* is not possible because it is

based purely on the dentition of *Ctenodus allodens*. This is in spite of there being relatively well-preserved skull material (NMS G. 1894.155.12, fig. 8, 9. Sharp & Clack, 2013). However, comparison with the skull material of *Ctenodus allodens* further discounts assigning *Limanichthys* to this genus and species on account of the anterolateral margin of the J-bone in *Ctenodus allodens* not contacting the posterior margin of the X-bone (fig. 8, 9, Sharp & Clack, 2013).

Delatitia was originally assigned to the genus *Ctenodus* by Woodward (1906) though was recognised by Long & Campbell (1985) as a separate genus on account of the structure of its long E-bones, the structure of the Y-bones as well as the course of the lateral line in the I-bone. The Y_1-bone in *Delatitia* is distinctive in possessing a characteristic embayment on the lateral margin to receive the operculum much as the X-bone does in *Limanichthys*. This embayment is, relative to *Delatitia*, positioned more anteriorly in *Limanichthys*. The identity of the lateral series of bones is confirmed by the second bone posterior to the X-bone (the Y_2-bone) lacking a bifurcation in the lateral line as would be expected if it were a Z-bone. Therefore this element is the Y_2-bone, the element anterior to that is the Y_1-bone followed by the X-bone. The fused X-Y_1-bone of *Sagenodus* possesses a similar embayment in an anterior position like that of *Limanicthys* in a fused X-Y_1-bone (interpreted by Schultze & Chorn, 1997, as a fused X-K-bone). *Limanichthys* also differs from *Sagenodus* in possessing a single anterior point of the B-bone rather than a double point (Fig. 3 C).

Sagenodus, *Ctenodus*, *Conchopoma* and *Uronemus* all possess a single F-bone anterior to the paired E-bones (Fig. 3 C-F respecitively). The specimen of *Limanichthys* described herein does not possess an F-bone but its presence cannot be ruled out as the most anterior part of the specimen is missing.

The course of the lateral line has previously been used as a means of discriminating dipnoan taxa and for homologising dermal bones (Stensiö 1947; Westoll 1949; White 1965; Lehman 1966; Schultze 1993) and we use the presence/absence of the various branches of the lateral line system to further distinguish between *Limanichthys* and *Ctenodus*. *Ctenodus allodens* possesses an anterior

lateral line groove in the B-bone which leads anterolaterally into the J-bone. *Limanichthys*, however, possesses no such groove. Furthermore, the lateral line in the I-bone of *Limanichthys* clearly displays pores rather than just a simple groove indicating that it is a continuation of the supraorbital lateral line from the Z-bone rather than a lateral line groove that traverses the I- to J-bones. The alignment of the lateral line pores in the I-bone and those in the Y_2-bone also preclude the continuity of the lateral line from the Y_2-bone to the I-bone.

The parasphenoid is phylogenetically informative in dipnoans (e. g. Marshall, 1986; Ahlberg *et* al. 2006; Clack *et al.* 2018) and so differences in the structure of this bone are of particular interest when comparing between taxa. A distinct ridge-groove is apparent on the corpus of the parasphenoid of *Ctenodus cristatus* (Sharp & Clack, 2013, fig. 16 A, B) on the buccal surface whereas the visceral surface of the stalk possesses a corrugated surface similar to *Limanichthys*. *Limanichthys*, however, lacks the distinctive lateral expansion of the parasphenoid stalk seen in *Ctenodus cristatus* (Fig. 4). The incomplete exposure of the stalk of the parasphenoid allows limited interpretation but from what can be seen the stalk possesses a single tapering point unlike the stalk of *Ctenodus cristatus* in which the stalk has a rounded posterior and distinct lateral expansions on the stalk. MicroCT scanning did not produce sufficient density contrast to segment the parasphenoid and reveal the complete structure of this bone.

Uronemus shares some superficial similarities with *Ctenodus* and *Limanichthys* in the arrangement of the skull roof bones as already mentioned. The D-bone, which has been demonstrated to be polymorphic in the Devonian forms *Dipterus*, *Scaumenacia* and *Pentlandia* (White 1965; Cloutier 1997; Challands & Den Blaauwen 2016) is considerably smaller in *Uronemus* (Fig. 3 F). *Limanichthys* possesses a single large D-bone as seen in *Ctenodus* but with a circular structure in the centre, a similar structure being present in the D-bone of *Sagenodus* and interpreted as a pit for the pineal organ (Schultze & Chorn 1997). Further differences between *Limanichthys* and *Uronemus* concern the characteristic surface ornamentation of the dermal bones

in the latter. Unlike *Uronemus splendens*, the external surface of the bone is not ornately sculpted with pits and ridges in *Limanichthys*. We do not consider that this ornamentation has been lost through erosion as the smooth nature of the surface is consistent across the entire specimen as lateral line pores are clearly evident.

Phylogenetic discussion

The interrelationships of Devonian and Carboniferous Dipnoi are unstable. This is reflected in topological disparity between previous analyses (Schultze & Chorn 1997; Lloyd *et al.* 2012; Pardo *et al.* 2014; Kemp *et al.* 2017) as well as low clade support for a monophyletic Carboniferous lungfish clade in the current analyses. However, several broad consistencies can be noted from both parsimony and Bayesian analyses of the Devonian and Carboniferous lungfish character matrix of this study: 1 – *Limanichthys* and *Delatitia* consistently resolve as basal members outside a monophyletic Carboniferous lungfish clade; 2 – some Carboniferous lungfish taxa (*Limanichthys* and *Delatitia*) consistently resolve within the Devonian phaneropleurid-fleurantiid grade; 3 – *Gnathorhiza*, *Palaeophichthys* and *Persephonichthys* consistently occupy a crownward position in the tree topology.

With all but a few exceptions (*Melanognathus*, *Sunwapta*, *Chirodipterus* and the dipnorhynchids), recent studies using a greater breadth of characters and taxa have established some stability within the Devonian taxa (Pardo *et al*. 2014; Challands & den Blaauwen, 2016). Similar efforts have not been spent in attempting to resolve the Carboniferous lungfish taxa with the recent exception of Kemp *et al*. (2017; Fig. 10 A) who produced an original character matrix that attempted to eliminate unknown character states for post-Devonian taxa. They included only well-known Carboniferous taxa at the generic level with two Devonian taxa (*Dipterus* and *Chirodipterus*) as the outgroup but crucially they also included post-Palaeozoic taxa. In particular, Kemp *et al*. (2017) drew attention to the previous use of dental characters in phylogenetic analyses

stating that characters concerned with tooth-ridge angle are inappropriate because they become modified during growth and from preservation. They also stated that the length to width ratio and number of ridges are unreliable as phylogenetic indicators as Kemp (1977) demonstrated that tooth ridge angle between individual ridges is indeed variable in both modern (*Neoceratodus*) and fossil (*Sagenodus*) taxa. One potential point of confusion here is with the definition of tooth ridge angle. In our analysis, we use tooth ridge angle as meaning the angle at the point subtended by the first and last tooth ridges, even if that point lies outside the tooth plate. This is not to be confused with the angle between *individual* tooth ridges which will change as more ridges are added to the tooth plate and as the tooth plate and ridges wear.

Though we do not dispute that intraspecific variation in length to width ratio and tooth ridge angle does occur, Smithson *et al*. (2015) were able to demonstrate the degree of interspecific variation is greater than the intraspecific variation in Late Devonian and Early Carboniferous lungfish tooth plates indicating that tooth ridge angle does hold important phylogenetic information. Furthermore, the bins for growth stages of *Sagenodus* in the data presented by Kemp (1977) are not continuous but have a gap of up to 10 x 6 mm between the definition of growth stages. This indicates that the data being presented do not represent a true growth continuum but the specimens chosen may in fact represent completely different taxa or the products of substantial remodelling and resorption that could abruptly alter morphology. Finally, in the study of Kemp (1977) where the number of measured tooth plate samples is low (ranging from 2 to 11 specimens for each growth stage of *Sagenodus*), the inferential power of the resulting statistics is low and, from central limits theorem, unlikely to represent the population mean.

Using their resulting post-Devonian phylogeny, Kemp *et al*. (2017) then created a compound phylogeny of Devonian and post-Devonian taxa by incorporating the result with that of Pardo *et al*. (2014). The analysis of Pardo *et al*. (2014) placed *Sagenodus* in a basal position among the phaneropleurids and fleurantiids but it also lacked the key Carboniferous taxon *Ctenodus*.

Incorporating *Ctenodus* into the phyologeny of Pardo *et al*. (2014) with the phylogenetic result of Kemp *et al*. (2017) would have produced a polytomy of ten taxa (*Ctenodus, Andreyevichthys, Scaumenacia, Adelargo, Sagenodus, Howidipterus, Barwickia, Fleurantia, Orlovichthys* and *Rhinodipterus kimberleyensis*). To avoid this Kemp *et al*. (2017) simply pruned *Ctenodus* out of their analysis. Such an approach, though convenient for producing a well-resolved tree for phylogenetic diversity estimates, gives a false impression of the compatibility between hypotheses of relationships for Devonian lungfish and Carboniferous lungfish using two entirely different character matrices. Our approach has been to use a comprehensive character matrix that includes many of the characters employed in the analysis of Kemp *et al*. (2017) but for as many Devonian and Carboniferous lungfish taxa as is feasible (based on completeness of specimens and suitable descriptions where specimens cannot be observed first hand). We have also included the well-preserved Permian taxon *Persephonichthys* (Pardo *et al*. 2014) which, when first described was placed as sister to the crown group lungfishses and, in turn, *Rhinodipterus kimberleyensis* and *Orlovichthys* were resolved as sisters to *Persephonichthys*. Such an approach with a great number of taxa is likely to result in polytomies and these are, to a degree, informative if only to demonstrate which taxa and associations are problematic.

Rhinodipterids. A monophyletic *Rhinodipterus* clade as recognised by Clement (2012) was disputed by Pardo *et al*. (2014) who considered *Rhinodipterus* to be a polyphyletic genus with *Rhinodipterus kimberleyensis* resolving as sister taxon to *Orlovichthys* and *Rhinodipterus ulrichi*, resolving in a more basal position below the 'phaneropleurid-fleurantiid' grade. The inclusion of *Phaneropleuron* creates instability in this clade in the parsimony analysis and collapses it to a polytomy. However, exclusion of *Phaneropleuron* results in *Rhinodipterus ulrichi*, *R. secans* and *R. kimberleyensis* being recovered as a monophyletic clade as in the analysis of Clement (2012) but also with the inclusion of *Celsiodon* (Clack *et al*. 2018). Bayesian analysis does not resolve a

significant monophyletic *Rhinodipterus* clade but does resolve *Celsiodon* in a more basal position as sister taxon to *Phaneropleuron*. The inclusion of the new Greenland taxon in this clade differs considerably from that of Clack *et* al. (2018) where it was recovered as sister taxon to *Ctenodus.* It is important to note, however, the changes made in the current matrix from that used in the analysis for *Celsiodon* (see supplementary information). Our analyses also confirm previous work proposing that the genus *Rhinodipterus* lies more crownward than *Dipterus* (Schultze 2001; Ahlberg *et al*. 2006; Friedman 2007b; Qiao & Zhu 2009).

Delatitia. In both our parsimony and Bayesian analyses *Delatitia* resolves within the phaneropleurid-fleurantiid grade (Figs. 8, 9). The parsimony hypothesis of Schultze & Chorn (1997, Fig. 10 E), wherein *Delatitia* is the most basal taxon of a monophyletic Carboniferous lungfish clade, is not reproduced here and our analysis is more similar to that of Lloyd *et al*. (2011, Fig. 10 F) in which *Delatitia* is a more basal member of the phaneropleurid-fleurantiid grade.

***Gnathorhiza* as a lepidosirenid**. The interpretation of *Gnathorhiza* as a stem lepidosirend is not new dating back as far as Case (1915), Romer & Smith (1934, who incidentally also listed several lines of evidence rejecting the association), and Olson & Daly (1972). However, earlier considerations of the inclusion of *Gnathorhiza* with the Lepidosirenidae were rejected primarily on grounds of convergence of tooth plate morphology by Stromer (1910) and later by Berman (1968), Schultze & Marshall (1997) and Schultze (2004). The phylogenetic analysis of Cavin *et al*. (2007) subsequently found *Gnathorhiza* to lie outside the Lepidosirenidae. They did not regard evidence pertaining to possible shared aestivation behaviour of the two groups as being conclusive for considering *Gnathorhiza* as a lepidosirenid. Most recently, however, Kemp *et al.* (2017) interpreted the gnathorhizids to be sister group to the lepidosirenids and included aestivation as a character for which they scored *Gnathorhiza* as being capable of making an aestivation burrow. In other taxa

where aestivation is marked as absent it is questionable how such a conclusion could have been derived.

The current analyses produce further interesting associations among the derived Carboniferous taxa. The introduction of the Permian lungfish *Persephonichthys* into the current analysis places *Persephonichthys* + *Palaeophichthys* as the sister taxa to *Gnathorhiza* similar to the analysis of Schultze (1994). The present study does not include the post-Carboniferous taxa included in Kemp *et al*. (2017) but *Gnathorhiza* consistently occupies a derived position monophyletic with *Palaeophicthys* and *Persephonichthys*.

In our phylogenetic review we have found that some of the characters coded for *Persephonichthys* in the matrix of Kemp *et al*. (2017) are incorrect . Firstly, Pardo *et al.* (2014, p. 5) describe three mediolateral bones in *Persephonichthys*; the KLM, J and I-bones rather than two or less as coded by Kemp *et al.* (2017). Pardo *et al.* (2014, p. 8) also clearly state the periorbital bones (Kemp *et al*. 2017, character 14) are incomplete in *Persephonichthys* and there is no evidence of the structure of the fins (Kemp *et al*. 2017, character 65). Although Pardo *et al*. (2014) identified scales in specimens of *Persephonichthys*, these data do not reveal any information about their structure or histology. As such, the characters mentioned above and characters 68, 70-72 of Kemp *et al*. (2017) should be coded as '?'. Rerunning a parsimony analysis under the conditions that Kemp *et al*. (2017) used produces three MPTs of length 163 but crucially *Gnathorhiza* + *Persephonichthys* consistently resolve above *Conchopoma* + *Uronemus* yet below all other post-Palaeozoic taxa. Furthermore, the tree collapses above *Gnathorhiza* + *Persephonichthys.* Conducting a Bayesian analysis of the corrected dataset of Kemp *et al*. (2017) resolves *Gnathorhiza* and *Persephonichthys* in a more basal position as in the corrected parsimony analysis (Fig. 10, C) placing it as the sister group to all post-Carboniferous lungfish and also reflecting the results of the analyses with our comprehensive character matrix (Fig. 9). The support for *Gnathorhiza* + *Persephonichthys* in the

Bayesian analysis with the corrected matrix is high (87%) with support for the node subtending the ceratodontids and lepidosirenids being low (44%).

Arguments in favour of or rejecting a clade on the basis of characters cannot be made for Bayesian analyses nor an analysis that does not include lepidosirenid taxa but in the light of our reanalysis of the data of Kemp *et al* (2017) and the position of *Gnathorhiza* and *Persephonichthys* in our analysis, we consider *Gnathorhiza* as being a lepidosirenid to be an unlikely natural association.

Persephonichthys as a transitional form. *Persephonichthys* was considered by Pardo *et al*. (2014) to be a transitional form between the dipterid grade lungfish and all modern lungfish though the most recent analysis of Carboniferous lungfish and post-Palaeozoic lungfish (Kemp *et al*. 2017) places *Persephonichthys* as a member of the lepidosirenid clade. *Persephonichthys* holds the same position in both the Bayesian and parsimony hypotheses in our analyses. Pardo *et al*. (2014) only included one Carboniferous taxon, *Sagenodus*, in their analysis but found *Persephonichthys* to resolve above *Rhinodipterus kimberleyensis* and below modern ceratodontiform lungfishes. Additionally, reanalysis of the Kemp *et al*. (2017) matrix (see above) also places *Persephonichthys* outside the lepidosirenid clade into a more basal position as a transitional form between Carboniferous and post-Palaeozoic lungfish rather than as a transitional form between the dipterid and modern lungfish as previously hypothesised by Pardo *et al*. (2014).

Conchopoma. *Conchopoma* is an unusual taxon with a mixture of both primitive and derived characters, as well as multistate characters, which has previously occupied an unstable position in phylogenetic analyses. Significant primitive characters in *Conchopoma* include a denticulated parasphenoid and a parasphenoid stalk with either a single or a bifid stalk (multistate) whereas derived characters of shared with more crownward taxa include the fusion of skull roof bones and

an uninterrupted median fin lacking a basal plate support (see supplemental information and matrix). The possession of both single and paired E-bones is another multistate character in *Conchopoma* that likely contributes to its instability. In our analyses *Conchopoma* and *Parasagenodus* are always resolved as sister taxa to each other though in polytomy in the Bayesian analysis. The poorly known *Parasagenodus* may be a contributing factor to the instability of this clade in the Bayesian analysis and previous analyses (Ahlberg *et al*. 2006). *Conchopoma* never resolves as sister taxon to *Uronemus* as in the analysis of Kemp *et al.* (2017). Our analysis places the node subtending *Conchopoma* + *Parasagenodus* towards the top of the tree (Figs 8, 9). This position in the Bayesian analysis has a posterior probability of 72% indicating the significance of this placement. The position of such 'transitional' forms as considered by (Kemp *et al.* 2017) is contentious yet important as, along with *Parasagenodus*, *Gnathorhiza*, *Palaeophichthys* and *Persephonichthys* (see above), they define what can be called the origin of 'modern' lungfish. If just the taxa included in the analysis of Kemp *et al.* (2017) are subject to parsimony analysis using our matrix, *Ctenodus* resolves in the same position as in Kemp *et al*. (2017). *Conchopoma*, however, then becomes sister taxon to the derived form *Gnathorhiza* and is placed at the top of the tree (Fig. 10 D) as Kemp *et al.* (2017) suspected may occur when characters applicable to both Palaeozoic and post-Palaeozoic lungfish (herein) are used.

Uronemus. *Uronemus* is considered as part of the Neodipnoi (see below) by Kemp *et al*. (2017) who considered it united with this group by possessing an ascending pterygopalatine process. On first-hand examination of the pterygoid of *Uronemus* NMS G 1976.19.3, no ascending pterygopalatine palatine process is seen to be present on the dorsal side of the specimen. A lateral thickening present on the posterolateral margin represents the thickened area between the upper jaw bone and the skull seen in Devonian lungfish as mentioned by Kemp *et al.* (2017) and demonstrates

some of the more primitive Devonian synapomorphies present in *Uronemus*. We do not consider *Uronemus* as a member of the Neodipnoi.

Neodipnoi. Our analysis thus brings into question the definition in Kemp *et al.* (2017) of the Neodipnoi; the clade including all taxa more closely related to *Lepidosiren*, *Neoceratodus*, *Gnathorhiza*, *Uronemus* and *Conchopoma* than to *Ctenodus* and *Sagenodus*. Adhering to the definition of Kemp *et al*. (2017) for the Neodipnoi and applying it to our parsimony analysis, the Neodipnoi would include all Carboniferous lungfish taxa other than *Sagenodus*, *Uronemus*, *Megapleuron*, *Xylognathus*, *Ctenodus*, *Delatita* and *Limanichthys.* The concept breaks down when considering the results of the Bayesian analysis where *Uronemus* resolves in a basal position in the Carboniferous lungfish clade and *Ctenodus* occupies a more derived position. The Neodipnoi are unified by, according to Kemp *et al*. (2017), among other characters, the presence of an ascending pterygopalatine process and lacking a gular series of bones albeit ambiguously because these characters are coded as unknown in *Conchopoma* and *Uronemus.* The lack of an ascending pterygopalatine process and associated structures (Kemp *et al*. 2017, supplementary information) in *Uronemus* (Smith et al., 1987, fig. 4 and see above), *Tranodis* and *Sagenodus* firmly dissociates these taxa from the Neodipnoi. *Conchopoma*, furthermore, possesses a complete complement of periorbital bones as figured by Marshall (1988, figs. 2, 3), the presence of which further removes this taxon from this definition of the Neodipnoi. Further problems with this definition are encountered specifically when considering *Tranodis* (Thomson 1966; Schultze & Bolt 1996). The lungfish *Tranodis* from the Upper Mississippian of North America, which was absent from the analysis of Kemp *et al*. (2017), occupies a derived position as primitive sister taxon to *Straitonia* in our parsimony analysis yet would not be included in the Neodipnoi under the definition of Kemp *et al.* (2017) as it possesses both a complete complement of periorbital bones and rostral bones anterior to the E-bones. *Palaeophichthys*, as sister taxon to *Gnathorhiza* and *Persephonichthys*, may

indeed possess an ascending pterygopalatine process from Schultze's (1994, p.109, fig. 2) description; "The posterior flange of the pterygoid has a steep medial side and a narrow width", but *Palaeophichthys* also possesses a gular series of bones. The legitimacy of *Palaeophichthys* as a valid genus is still debated and it has been considered a synonym of *Monongahela* (Schultze 1994) yet is also considered a distinct genus by Kemp (1998). In our analysis we have coded *Palaeophichthys* from the descriptions provided by Eastman (1908, 1917) and Schultze (1994) and retrieve the close association of *Gnathorhiza* and *Palaeophichthys* that Miles (1977), Schultze (1994) and Schultze & Marshall (1993) found.

Given these inconsistencies we regard the included taxa of the Neodipnoi as proposed by Kemp *et al.* (2017) as not being valid and adopt the original definition of Agnolin (2010) as the Neoceratodontidae + Lepidosirenidae.

Dipnoan size following the Hangenberg extinction event. Sallan & Galimberti (2015) compiled an extensive dataset of the size of all vertebrate taxa that existed across the Devonian-Carboniferous boundary and employed regression analyses to ascertain if there was any significant decline in size of taxa following the Hangenberg extinction event. In essence they were testing for the Lilliput effect (Urbanek 1993) as has been recognised in invertebrate taxa following the end-Permian extinction (Twitchett 2007) and terrestrial vertebrate taxa (Huttenlocker, 2014). Their data were based on estimated body size from reconstructions in the published literature from which they demonstrated that there was a slight decrease in size of all vertebrate taxa from the Devonian into the Carboniferous. Dipnoan size was shown to remain static throughout the Carboniferous without any statistical increase or decrease in body length.

The estimated body sizes of the lungfish discovered recently in the Tournaisian of the Scottish Borders and Midland Valley (Carpenter *et al.* 2014, Challands *et al.* 2015, Smithson *et al.* 2015 and this present study) are broadly consistent with the pattern expected from Sallan and

Galimberti's (2015) analysis. *Limanichthys*, from the earliest Carboniferous, at c. 34.5 m above the D/C boundary, and less than 0.5 million years after the Hangenberg event, is a relatively large fish, at least 150 cm long. It is the largest of all the lungfish taxa collected from the horizons in the lower half of the Tournaisian. This includes specimens from Bute (Carpenter *et al*. 2014), Willie's Hole and most of the other material from Burnmouth (Smithson *et al.* 2012, 2016 Clack *et al.* 2016, Otoo *et al*. 2018). Evidence of much larger taxa has been found in the highest tetrapod-bearing horizon at Burnmouth (Clack *et al.* 2016, Clack *et al*. 2019) with individual bones representing lungfish up to 3 m long. In contrast, remains of very small individuals have been collected throughout the Ballagan Formation representing fish no more than 10 cm long. The majority were probably less than 40 cm long which may be indicative of the Lilliput effect (Sallan & Galimberti 2016). The phylogenetic analysis suggests that the largest Tournaisian taxa (*Limanichthy* and *Delatitia*) belong to lungfish clades with their roots deep in the Devonian and that the smaller taxa (e.g. *Xylognathus* and *Sagenodus*) represent part of a new radiation of post-Hangenberg lungfish, a trend which apparently continued throughout the Mississippian (Smithson *et al.* in press)

Carboniferous radiation of lungfish. Elucidating a cause for this new radiation in lungfish, as well as why a Devonian group persisted into the Carboniferous is problematic. Sallan & Coates (2010) suggested that piscine sarcopterygians underwent a taxic decline in the aftermath of the Hangenberg extinction event and further stated that marine and freshwater environments were affected equally. Our results show that freshwater and brackish lineages from within the phaneropleurid – fleurantiid grade survived the Hangenberg extinction event. Our data also imply that the roots of some of these lineages (e.g. *Limanichthys*, *Delatitia*) lie deep within the Devonian rather than being a purely Carboniferous innovation. Tooth plates assigned to *Limanichhthys* and *Delatitia* are not known (those reported by Long & Campbell, 1985, for *Delatitia* are incomplete and not associated directly with the cranial material) but recently two undescribed tooth plates from

the Frasnian of Russia have been found to possess characteristics similar to *Ctenodus* toothplates, namely ovate shape, parallel ridges, a convex prearticular tooth plate surface and a tooth ridge angle less than 40º (Challands *et al*. 2017) indicating at least a possible Devonian origination for other Carboniferous taxa. The Carboniferous lungfish of the phaneropleurid – fleurantiid grade (*Limanichthys* and *Delatitia*) may therefore represent a 'dead clade walking' (Jablonski 2002) being the last of the phaneropleurid – fleurantiid association and not part of a distinct Carboniferous lungfish radiation. Rather, we suggest that the Carboniferous lungfish radiation *sensu stricto* is represented by forms possessing, in particular, high tooth ridge angles with fusion of cusps and fewer tooth rows and with reduced dermal ossifications that represent transitional forms prior to the advent of the Ceratodontoidei. We consider the Ceratodontoidei to comprise the clade including all taxa more closely related to *Lepidosiren* and *Neoceratodus* than to *Palaeophichthys* and *Persephonichthys*.

Persephonichthys was found by Pardo *et al.* (2014) to possess a pectoral girdle structure that, unlike other Carboniferous lungfish, was decoupled from the skull, as in extant lungfish. From this they inferred that *Persephonichthys* was capable of an improvement in feeding through buccal suction though suction feeding was demonstrated by Clement *et al*. (2016) to already be manifest in Devonian taxa as demonstrated by the pectoral girdle of *Rhinodipterus*. As well as being a Permian form, our analyses suggest that *Persephonichthys* plus crown lungfishes represent descendents of the Carboniferous radiation rather than being derived from Devonian phaneropleurid-fleurantiid stock. In such a case, the development of a skeletal mechanism capable of buccal pumping for suction feeding (as indicated by the presence of a long posterior parasphenoid stalk and the presence of large cranial ribs) must have occurred during or after (unlikely) the development of new tooth plate morphologies. The tooth plates of *Persephonichthys* possess a high tooth ridge angle, with laterally compressed ridges and only four tooth rows. Additionally, the first tooth row of *Persephonichthys* is extremely elongate relative to the other two rows, a feature that is also present

in *Gnathorhiza dikeloda*. Such features are typical of many Early Carboniferous lungfishes (e.g *Xylognathus*, *Uronemus*, *Coccovedus*, *Occludus*) but are also present to a lesser degree in some stemward lungfish including *Orlovichthys* and *Rhinodipterus.* This likely represents a certain degree of heterodonty in lungfish, in which the elongate and laterally compressed first tooth row function differently during occlusion from the other rows (Smithson *et al*. in press). The Carboniferous lungfish radiation therefore appears to represent a wholesale, concomittant adoption of novel mastication strategies and food capture (suction feeding) first seen in a handful of Devonian taxa but becoming prevalent during a time of significant environmental change following the Hangenberg event.

The onset of the Carboniferous saw a profound change in habitats that sarcopterygians, both piscine and tetrapod, occupied. Anderson *et al*. (2015) and Clack *et al*. (2016) were able to demonstrate that tetrapod diversification was well underway by the Tournaisian. At this time there were diverse wetland environments and seasonal palaeosols in coastal floodplains in the region subsequently represented by the Scottish Borders (Kearsey *et al.* 2016). Such environments were not exclusively freshwater as indicated by Kearsey *et al.* (2016) as well as trace-fossils (Bennett *et al*. 2017) and gypsum/anhydrite evaporites (Millward *et al.* 2018). Together these data provide evidence of marine-to-brackish water input onto the floodplain. Floodplain lakes contained a diverse vertebrate fauna besides lungfish (rhizodonts, tetrapods, actinopterygians, chondrichthyans). Invertebrate fossils include ostracods (*Shemonaella* and *Paraparchites*), bivalves (*Modiolus* and *Naiadites*) and rare eurypterids, shrimps, *Spirorbis* sp. *Serpula* sp., orthocones and scolecodonts (Bennett *et al*. 2016, Otoo *et al.* 2018). No direct evidence has been found indicating the diet of different Palaeozoic lungfish though they are generally considered to have been durophagous (Clement *et al*. 2016). The innovations in the pectoral girdle outlined by Pardo *et al*. (2014) represented a change to a more varied omnivorous feeding strategy. The prevalence of plant material in the Ballagan Formation coupled with the abundance of small actinopterygian fish (Otoo

et al. 2018) and the diversity and innovations in lungfish tooth plate morpholgies encountered in the Tournaisian (Smithson *et al.* 2015) may indicate a more varied diet in some of the lungfish at this time compared to lungfish from the Devonian. The diversity of new ecological niches in the Tournaisian Ballagan Formation represents a step change from the relatively uniform environments of the marine realm or large lacustrine habitats (e.g. the Orcadian Basin of Scotland) predominant in the Devonian and it is into these environments that both Devonian lungfish survivors and the new Carboniferous lungfish clade radiated.

Conclusions

Limanichtys fraseri is the earliest lungfish recovered from Carboniferous strata immediately following the Devonian Hangenberg extinction event. Phylogenetic analysis resolves *Limanichthys* with the primitive Devonian lungfish *Pentlandia* in a separate, more basal clade than the majority of other Carboniferous lungfish. Both parsimony and Bayesian analyses imply deep roots for certain Carboniferous taxa from the phaneropleurid-fleurantiid grade lungfish with *Limanichthys* and *Delatitia* possibly representing relict taxa from within this grade. The inclusion of Carboniferous lungfish alongside Devonian forms blurs the boundaries of what are formerly considered ‘Devonian’ or ‘Carboniferous’ lungfish clades. Separate from this mixture of Devonian and Carboniferous taxa, a unique radiation of exclusively Carboniferous lungfish occurred before the advent of the Ceratodontoidei and Neodipnoi *sensu* Agnolin (2010). This radiation is typified by lungfish with heterodont tooth plates with a reduced number of tooth ridges and laterally compressed tooth rows that likely represent a response to the diversification of ecological niches that became available in seasonally wet-dry brackish to freshwater coastal flood plain environments in the Tourniasian. These data indicate that the Hangenberg extinction was not environmentally

pandemic and some taxa of Devonian stock that inhabited non-marine environments survived into the Carboniferous as dead clades walking, joining the likes of the rhizodonts.

Acknowledgements

The authors would like to thank Anne Brown and Colin MacFadyan at Scottish Natural Heritage and Paul Bancks at the Edinburgh office of The Crown Estate Scotland for permission to collect at Burnmouth, Dr Stig Walsh (National Museums Scotland) for the loan of specimens and access to the collections at National Museums Scotland; Keturah Smithson (University Museum of Zoology Cambridge) for microCT scanning. Two reviewers, Jason Pardo and Dr Alice Clement provided valuable suggestions that have greatly improved the manuscript. This work was carried out with the aid of NERC consortium grants NE/J022713/1 (Cambridge), NE/J020729/1 (Leicester) and NE/J021091/1 (Southampton). Tom Challands acknowledges financial support from Callidus Services Ltd.

References

Agnolin, F. 2010. A new species of the genus *Atlantoceratodus* (Dipnoiformes:Ceratodontidei) from the uppermost Cretaceous of Patagonia and brief overview of fossil dipnoans from the Cretaceous and Paleogene of South America. *Brazilian Geographical Journal: Geosciences and Humanities Research Medium*. **1**, 162–210.

Ahlberg, P. E. 1991. A re-examination of sarcopterygian interrelationships, with special reference to the Porolepiformes. *Zoological Journal of the Linnean Society*, **103**(3), 241-287.

Ahlberg, P. E. Smith, M. M. & Johanson, Z., 2006. Developmental plasticity and disparity in early dipnoan (lungfish) dentitions. *Evolution & development*, **8**(4), 331-349.

Anderson, J. S., Smithson, T., Mansky, C. F., Meyer, T. and Clack, J., 2015. A Diverse Tetrapod Fauna at the Base of'Romer's Gap'. *PloS one*, **10**(4), p.e0125446. doi.org/10.1371/journal.pone.0125446

Bemis, W. E. 1984. Morphology and growth of lepidosirenid lungfish tooth plates (Pisces: Dipnoi). *Journal of Morphology*, **179**(1), 73-93.

Bennett, C. E., Kearsey, T. I., Davies, S. J., Millward, D., Clack, J. A., Smithson, T. R. & Marshall, J. E. 2016. Early Mississippian sandy siltstones preserve rare vertebrate fossils in seasonal flooding episodes. *Sedimentology*, **63**(6), 1677-1700.

Bennett, C. E., Howard, A. S. H., Davies, S. J., Kearsey, T. I., Millward, D., Brand, P. J., Browne, M. A. E., Reeves, E. J. & Marshall, J. E. A. 2017. Ichnofauna record cryptic marine incursions onto a coastal floodplain at a key early Mississippian tetrapod site. P*alaeogeography, Palaeoclimatology, Palaeoecology*, **468**, 287-300.

Berman, D.S. 1968. Lungfish from the Lueders Formation (Lower Permian, Texas) and the Gnathorhiza-lepidosirenid ancestry questioned. *Journal of Paleontology*, **42**(3), 827-835.

Carpenter, D. K., Falcon-Lang, H. J., Benton, M. J. & Henderson, E. 2014. Carboniferous (Tournaisian) fish assemblages from the Isle of Bute, Scotland: systematics and palaeoecology. *Palaeontology*, **57**(6), 1215-1240.

Cavin, L., Suteethorn, V., Buffetaut, E. & Tong, H. 2007. A new Thai Mesozoic lungfish (Sarcopterygii, Dipnoi) with an insight into post-Palaeozoic dipnoan evolution. *Zoological Journal of the Linnean Society*, **149**, 141-177

Challands, T. J., Bennett, C.E., Clack, J. A., Fraser, N., Kearsey,T. I., Marshall, J. E.A., Smithson, T. R. & Walsh, S. A. 2015. The Tournaisian: a sarcopterygian incubator. In 59th Annual Meeting of the Palaeontological Association Abstracts, 57. http://www.palass.org/meetings-events/annual-meeting/2015/annual-meeting-2015-cardiff-poster-abstracts

Challands, T. J. & Den Blaauwen, J. 2016. A redescription of the Middle Devonian dipnoan *Pentlandia macroptera* Traquair, 1889, and an assessment of the Phaneropleuridae. *Zoological Journal of the Linnean Society*, **180**(2), 414-460.

Challands, T., Lebedev, O., Friedman, M. & Krupina, N. 2017. A case of mistaken identity:'*Latvius' obrutus* and new dipnoans from the Frasnian of Stolbovo, Russia (No. e3231v1). *PeerJ Preprints*. doi.org/10.7287/peerj.preprints.3231v1

Clack, J. A., Bennett, C. E., Carpenter, D. K., Davies, S. J., Fraser, N. C., Kearsey, T. I., Marshall, J. E., Millward, D., Otoo, B. K., Reeves, E. J., Ross, A. J., Ruta, M., Smithson, K. Z., Smithson, T. R. & Walsh, S. A. 2016. Phylogenetic and environmental context of a Tournaisian tetrapod fauna. *Nature Ecology & Evolution*, **1**, p.0002. doi:10.1038/s41559-016-0002

Clack, J. A., Challands, T. J., Smithson, T. R., Smithson, K. Z. 2018. Newly recognized Famennian lungfishes from east Greenland reveal tooth plate diversity and blur the Devonian-Carboniferous boundary. *Papers in Palaeontology.* doi.org/10.1002/spp2.1242

Clack, J. A., Bennett, C. E., Davies, S. J., Scott, A. C., Sherwin, J. and Smithson, T. R. 2019. A Tournaisian (earliest Carboniferous) conglomerate-preserved non-marine faunal assemblage and its environmental and sedimentological context. *PeerJ* **6**:e5972. doi.org/10.7717/peerj.5972

Clement, A.M. 2012. A new species of long-snouted lungfish from the Late Devonian of Australia, and its functional and biogeographical implications. *Palaeontology*, **55**(1), 51-71.

Clement, A. M., Long, J. A., Tafforeau, P. & Ahlberg, P. E. 2016. The dipnoan buccal pump reconstructed in 3D and implications for air breathing in Devonian lungfishes. *Paleobiology*, **42**(2), 289-304.

Cloutier, R. 1997. Morphologie et variations du toit crânien du dipneuste *Scaumenacia curta* Whiteaves (Sarcopterygii), du Dévonien supérieur du Québec. *Geodiversitas*, **19** (1), 61-105.

Cope, E. D. 1877. Descriptions of extinct Vertebrata from the Permian and Triassic Formamations of the United States. *Proceedings of the American Philosophical Society*, **17**(100), 182-193.

Forster-Cooper, C. 1937. VII.—The Middle Devonian Fish Fauna of Achanarras. *Transactions of The Royal Society of Edinburgh*, **59**(1), 223-239.

Friedman, M. 2007a. Cranial structure in the Devonian lungfish *Soederberghia groenlandica* and its implications for the interrelationships of 'rhynchodipterids'. *Earth and Environmental Science Transactions of the Royal Society of Edinburgh*, **98**(2), 179-198.

Friedman, M. 2007b. The interrelationships of Devonian lungfishes (Sarcopterygii: Dipnoi) as inferred from neurocranial evidence and new data from the genus *Soederberghia* Lehman, 1959. *Zoological Journal of the Linnean Society*, **151**(1), 115-171.

Friedman, M. & Sallan, L. C. 2012. Five hundred million years of extinction and recovery: a Phanerozoic survey of large-scale diversity patterns in fishes. *Palaeontology*, **55**(4), 707-742.

Goloboff, P. A., Farris, J. S. & Nixon, K. C. 2008. TNT, a free program for phylogenetic analysis. *Cladistics*, **24**(5), 774-786.

Huxley, T. H. 1880. On the application of the laws of evolution to the arrangement of the Vertebrata, and more particularly of the Mammalia. *Proceedings of the Zoological Society, London* **43,** 649-662

Huttenlocker, A. K. 2014. Body size reductions in nonmammalian eutheriodont therapsids (Synapsida) during the end-Permian mass extinction. *PLoS One*, *9*(2), p.e87553. doi.org/10.1371/journal.pone.0087553

Jablonski, D. 2002. Survival without recovery after mass extinctions. *Proceedings of the National Academy of Sciences*, USA, **99**, 8139–8144.

Jarvik, E. 1967. On the structure of the lower jaw in dipnoans: with a description of an early Devonian dipnoan from Canada, *Melanognathus canadenis* gen. et sp. nov. *Zoological Journal of the Linnean Society*, **47**(311), 155-183.

Kaiser, S. I., Aretz, M. and Becker, R. T. 2016. The global Hangenberg Crisis (Devonian–Carboniferous transition): review of a first-order mass extinction. *Geological Society, London, Special Publications*, **423**, 387-437.

Kearsey, T. I., Bennett, C. E., Millward, D., Davies, S. J., Gowing, C. J., Kemp, S. J., Leng, M. J., Marshall, J. E. A. & Browne, M. A. 2016. The terrestrial landscapes of tetrapod evolution in earliest Carboniferous seasonal wetlands of SE Scotland. *Palaeogeography, Palaeoclimatology, Palaeoecology*, **457**, 52-69.

Kemp, A. 1977. The pattern of tooth plate formation in the Australian lungfish, *Neoceratodus forsteri* Krefft. *Zoological Journal of the Linnean Society*, **60**(3), 223-258.

Kemp, A., Cavin, L. & Guinot, G. 2017. Evolutionary history of lungfishes with a new phylogeny of post-Devonian genera. *Palaeogeography, Palaeoclimatology, Palaeoecology*, **471**, 209-219.

Krupina, N. I. & Reisz, R. R. 1999. Reconstruction of dentition in hatchlings of *Andreyevichthys epitomus*, a late Famennian dipnoan from Russia. *Modern Geology*, **24**(1), 99.

Lehman J.-P. 1959. Les dipnuestes du Dévonien supérieur du Groenland. *Meddelelser om Grønland*, **160**(4), 1–58.

Lloyd, G. T., Wang, S. C. & Brusatte, S. L. 2012. Identifying heterogeneity in rates of morphological evolution: discrete character change in the evolution of lungfish (Sarcopterygii; Dipnoi). *Evolution*, **66**(2), 330-348.

Long, J. A. 1992. Cranial anatomy of two new late Devonian lungfishes (Pisces: Dipnoi) from Mount Howitt, Victoria. *Records of the Australian Museum*, **44**(3), 299-318.

Long, J. A. & Campbell, K. S. W. 1985. A new lungfish from the Lower Carboniferous of Victoria, Australia. *Proceedings of the Royal Society of Victoria*, **97**(2), 87-93.

Marshall, C. R. 1986. Lungfish: phylogeny and parsimony. *Journal of Morphology*, **190**(S1), 151-162.

Marshall, C. R. 1988. A large, well preserved specimen of the Middle Pennsylvanian lungfish *Conchopoma edesi* (Osteichthyes: Dipnoi) from Mazon Creek, Illinois, USA. *Journal of Vertebrate Paleontology*, **8**(4), 383-394

Marshall, J. E. A., Reeves, E. J., Bennet, C. E., Davies, S. J., Kearsey, T. I., Millward, D., Smithson, T. R. & Browne, M. A. E. In press. Reinterpreting the age of the uppermost 'Old Red Sandstone' and Early Carboniferous in Scotland. *Earth and Environmental Science Transactions of the Royal Society of Edinburgh.*

Miles, R. S. 1977. Dipnoan (lungfish) skulls and the relationships of the group: a study based on new species from the Devonian of Australia. *Zoological Journal of the Linnean Society*, **61**(1-3), 1-328.

Millward, D., Davies, S. J., Williamson, F., Curtis, R., Kearsey, T. I., Bennett, C. E., Marshall, J. E. and Browne, M. A., 2018. Early Mississippian evaporites of coastal tropical wetlands. *Sedimentology*, **65**(7), doi:10.1111/sed.12465

Müller, J. 1845. Über den Bau und die Grenzen der Ganoiden und das natürliche System der Fische. *Abhandlungen der Akademie der Wissenschaften zu Berlin*, **1845**: 117–216.

Olson, E. C. 1951. Fauna of Upper Vale and Choza. 3. Lungfish of the Vale 4. The skull of *Gnathorhiza dikeloda* Olson. *Fieldiana: Geology (Chicago)*, **10,** 104-124.

Olson, E. C. & Daly, E. 1972. Notes on *Gnathorhiza* (Osteichthyes, Dipnoi). *Journal of Paleontology*, 46(3), 371-376.

Ørvig, T. 1961. New finds of acanthodians, arthrodires, crossopterygians, ganoids and dipnoans in the upper Middle Devonian calcareous flags (Oberer Plattenkalk) of the Bergisch Gladbach-Paffrath trough. *Paläontologische Zeitschrift*, **35**(1-2), 10-27.

Otoo, B. K. A., Clack, J. A., Smithson, T. R., Bennett, C. E., Kearsey, T. I., Coates, M. I. 2018. A fish and tetrapod fauna from Romer's Gap preserved in Scottish Tournaisian floodplain deposits. *Palaeontology*. doi:10.1111/pala.12395

Pardo, J. D., Huttenlocker, A. K. & Small, B. J. 2014. An exceptionally preserved transitional lungfish from the Lower Permian of Nebraska, USA, and the origin of modern lungfishes. *PloS one*, **9**(9), p.e108542. doi.org/10.1371/journal.pone.0108542

Qiao, T. & Zhu, M. 2009. A new tooth-plated lungfish from the Middle Devonian of Yunnan, China, and its phylogenetic relationships. *Acta Zoologica*, **90**(s1), 236-252.

Qiao, T. & Zhu, M. 2015. A new Early Devonian lungfish from Guangxi, China, and its palaeogeographic significance. *Alcheringa: An Australasian Journal of Palaeontology*, **39**(3), 428-437.

Romer, A. S. 1955. Herpetichthyes, Amphibioidei, Choanichthyes or Sarcopterygii?. *Nature*, **176**(4472), 126.

Sallan, L. C. & Coates, M. I. 2010. End-Devonian extinction and a bottleneck in the early evolution of modern jawed vertebrates. *Proceedings of the National Academy of Sciences*, **107**(22), 10131-10135.

Sallan, L. & Galimberti, A. K. 2015. Body-size reduction in vertebrates following the end-Devonian mass extinction. *Science*, **350**(6262), 812-815.

Schindelin, J., Arganda-Carreras, I., Frise, E., Kaynig, V., Longair, M., Pietzsch, T., Preibisch, S., Rueden, C., Saalfeld, S., Schmid, B. & Tinevez, J. Y. 2012. Fiji: an open-source platform for biological-image analysis. *Nature methods*, **9**(7), 676-682.

Schultze, H. -P. 1993 Skull of jawed fishes. Pp. 189-254. in Hanken J. & Hall B. K. (eds) *The Skull Volume 2: Patterns of Structural and Systematic Diversity*. University of Chicago Press.

Schultze, H. -P. 1994. *Palaeophichthys parvulus* Eastman, 1908, a gnathorhizid dipnoan from the Middle Pennsylvanian of Illinois, USA. *Annals of the Carnegie Museum*, **63**, 105-13.

Schultze, H. -P. 2001. *Melanognathus*, a primitive dipnoan from the Lower Devonian of the Canadian Arctic and the interrelationships of Devonian dipnoans. *Journal of Vertebrate Paleontology*, **21**(4), 781-794.

Schultze, H. -P. & Bolt, J.R., 1996. The lungfish *Tranodis* and the tetrapod fauna from the Upper Mississippian of North America. *Special Papers in Palaeontology*, **52**, 31-54.

Schultze, H. -P. & Chorn, J. 1997. The Permo-Carboniferous genus *Sagenodus* and the beginning of modern lungfish. *Contributions to Zoology*, **67**(1), 9-70.

Schultze, H. -P. & Marshall, C. R. 1993. Contrasting the use of functional complexes and isolated characters in lungfish evolution. *Memoirs of the Association of Australasian Palaeontologists*, **15**, 211-224.

Skrzycki, P. 2016. The westernmost occurrence of *Gnathorhiza* in the Triassic, with a discussion of the stratigraphic and palaeogeographic distribution of the genus. *Mitteilungen aus dem Museum für Naturkunde in Berlin. Fossil Record*, **19**(1), 17.

Sharp, E. L. & Clack, J. A. 2013. A review of the Carboniferous lungfish genus *Ctenodus* Agassiz, 1838 from the United Kingdom, with new data from an articulated specimen of *Ctenodus* interruptus Barkas, 1869. *Earth and Environmental Science Transactions of the Royal Society of Edinburgh*, **104**(2), 169-204.

Smith, M. M., Smithson, T. R. & Campbell, K. S. W. 1987. The relationships of *Uronemus*: a Carboniferous dipnoan with highly modified tooth plates. *Phil. Trans. R. Soc. Lond. B*, *317*(1185), 299-327.

Smithson, T. R., Wood, S. P., Marshall, J. E. & Clack, J. A. 2012. Earliest Carboniferous tetrapod and arthropod faunas from Scotland populate Romer's Gap. *Proceedings of the National Academy of Sciences*, **109**(12), 4532-4537.

Smithson, T. R., Richards, K. R. & Clack, J. A. 2015. Lungfish diversity in Romer's Gap: reaction to the end-Devonian extinction. *Palaeontology*, **59**(1), 29-44.

Smithson, T. R., Challands, T. J. & Smithson, K. Z. In press. Traquair's lungfish from Loanhead: dipnoan diversity and tooth plate growth in the late Mississippian. *Earth and Environmental Science Transactions of The Royal Society of Edinburgh.*

Stensiö, E. A. 1947. The sensory lines and dermal bones of the cheek in fishes and amphibians. *Kungliga Svenska Vetenskapsakademiens Handlingar*, **24**, 1-195.

Stromer E. 1910. Ueber das Gebiss des Lepidosirenidae und die Verbreitung tertiärer und mesozoischer Lungenfische. Festschrift zum 60 Geburtstage der R Hertwigs, band 2, Jena : 611 – 625.

Thomson, K. S. 1965. On the relationships of certain Carboniferous Dipnoi; with the description of four new forms. *Proceedings of the Royal Society of Edinburgh Section B (Biology)* **69**, 221-45.

Traquair, R. H. 1871. I.—Notes on the Genus *Phaneropleuron* (Huxley), with a description of a new species from the Carboniferous Formation. *Geological Magazine*, **8**(90), 529-535.

Twitchett, R. J. 2007. The Lilliput effect in the aftermath of the end-Permian extinction event. *Palaeogeography, Palaeoclimatology, Palaeoecology*, **252**(1), 132-144.

Urbanek, A. 1993. Biotic crises in the history of Upper Silurian graptoloids: a palaeobiological model. *Historical Biology*, **7**, 29–50.

Watson, D. M. S. & Gill, E. L. 1923. The structure of certain Palaeozoic Dipnoi. *Journal of the Linnean Society of London, Zoology*, **35**(233), 163-216.

Westoll, T. S. 1949. On the evolution of the Dipnoi. Pp. 112-184 in Jepson, G. L., Mayr, E. & Simpson, G. G. (eds) *Genetics, paleontology and evolution.* Princeton University Press.

White, E. I. 1965. The head of *Dipterus valenciennesi* Sedgwick & Murchison. *Bulletin of the British Museum (Natural History), Geology*, **11**, 1-45.

Wilkinson, M. 1995. Coping with abundant missing entries in phylogenetic inference using parsimony. *Systematic Biology*, **44**(4), 501-514.

Woodward, A. S. 1906. On a Carboniferous fish fauna from the Mansfield District, Victoria. *Memoirs of the National Museum, Melbourne*. **1**, 1-32.

Young, G. C. & Schultze, H. -P. 2005. New osteichthyans (bony fishes) from the Devonian of Central Australia. *Fossil Record*, **8**(1), 13-35.

Figure 1. Distribution of the Ballagan Formation in south eastern Scotland and north eastern England and stratigraphic position of *Limanichthys* in the section of the Ballagan Formation at Burnmouth. Sedimentary log redrawn from Kearsey *et al*. (2016).

Figure 2. Counterpart (**A**) and part (**B**) of NMS G 2017.10.2 with respective interpretive drawings (**C, D**) showing the identified skull roof bones and parasphenoid.

Figure 3. Reconstructions of Devonian and Carboniferous dipnoan skull roofs: A**.** *Limanichthys fraseri*; **B**. *Pentlandia macroptera*; **C**. *Sagenodus inaequalis*; **D**. *Ctenodus allodens*; **E**. *Conchopoma gadiforme*; **F**. *Uronemus splendens.* **B** after Challands & Den Blaauwen (2016); **D** after Westoll (1949) and Sharp & Clack (2013); **C**, **E** & **F** after Westoll (1949).

Figure 4. A. Parasphenoid of *Limanichthys fraseri* in the part specimen showing impression of parasphenoid stalk and posterior region of lateral expansion of the corpus; **B**. Stalk of parasphenoid of *Limanichthys* showing strong ridging and tapering to a single point; **C**. Tentative reconstruction of the parasphenoid of *Limanichthys*; **D**. Parasphenoid of *Sagenodus copenanus* in visceral view from Schultze & Chorn (1997) fig. 22; **E**. Parasphenoid of *Ctenodus interruptus* in visceral view from Watson & Gill (1923), fig. 25 b; **F**. Parasphenoid of *Ctenodus cristatus*, buccal view, from Sharp & Clack (2013), fig. 15 b; **G**. Parasphenoid of *Pentlandia macroptera* from Challands & Den Blaauwen (2016), fig. 5 a. Scale bars: **A**-**F** = 10 mm, G = 4 mm.

Figure 5. A. UMZC 2017.5.10a-c showing disarticulated operculum, ribs, cranial ribs, anocleithra and tooth plate of *Limanichthys*; **B**. Interpretive drawing of skeletal elements in UMZC 2017.5.10a-c. Scale bars = 50 mm.

Figure 6. A. MicroCT rendering of NMS G 2017.10.2a with translucent mask showing position of the marginal tooth plate of *Limanichthys* below the parasphenoid. **B**. Detailed rendering of the marginal tooth plate exhibiting seven individual cusps that decrease in size to the posterior (right).

Figure 7. Detail of tooth plate and anocleithrum on UMZC 2017.5.10c. Scale bar = 10 mm.

Figure 8. Strict consensus tree from 27 most parsimonious trees (length = 898, CI = 0.28, RI = 0.60). Values next to nodes represent Bremer support indices. Carboniferous taxa are shown in grey boxes.

Figure 9. 50% majority rule tree from Bayesian analysis. Posterior probabilities >50% are shown next to nodes. Carboniferous taxa are shown in grey boxes.

Figure 10. Different phylogenetic hypotheses for Devonian, Carboniferous and post-Palaeozoic lungfish. **A**. Analysis of Kemp *et al*. (2017) placing *Gnathorhiza* with the lepidosirenids; **B**. 50% consensus tree (length 176) of 5 MPT (length 175) for reanalysis of the matrix of Kemp *et al*. (2017) following correction of character codings for *Persephonichthys*. *Gnathorhiza* resolves well outside the lepidosirenids as the most derived Carboniferous taxon; **C**. Bayesian analysis of the corrected matrix of Kemp *et al*. (2017) that also resolves *Gnathorhiza* outside the lepidosirenids; **D**. Phylogeny of matrix used in this study only including the taxa used present in the matrix of Kemp *et al*. (2017). *Conchopoma* resolves in a derived position in the crown rather than in a basal position; **E**. Hypothesis of Schultze & Chorn (1997) with *Conchopoma* resolving in a basal position; **F**. Hypothesis of Lloyd et al. (2012) with *Conchopoma* resolving in a basal position and *Gnathorhiza* resolving as the sister to all post-Palaeozoic taxa as per the current analysis.

Figure 1

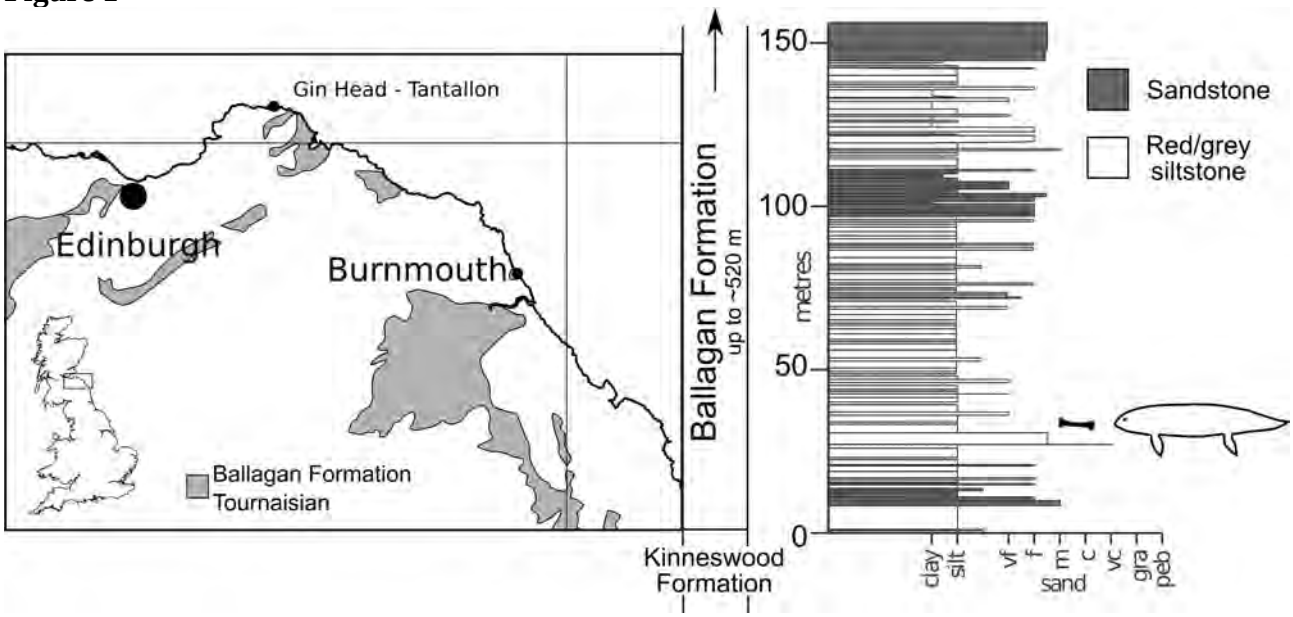

Figure 2

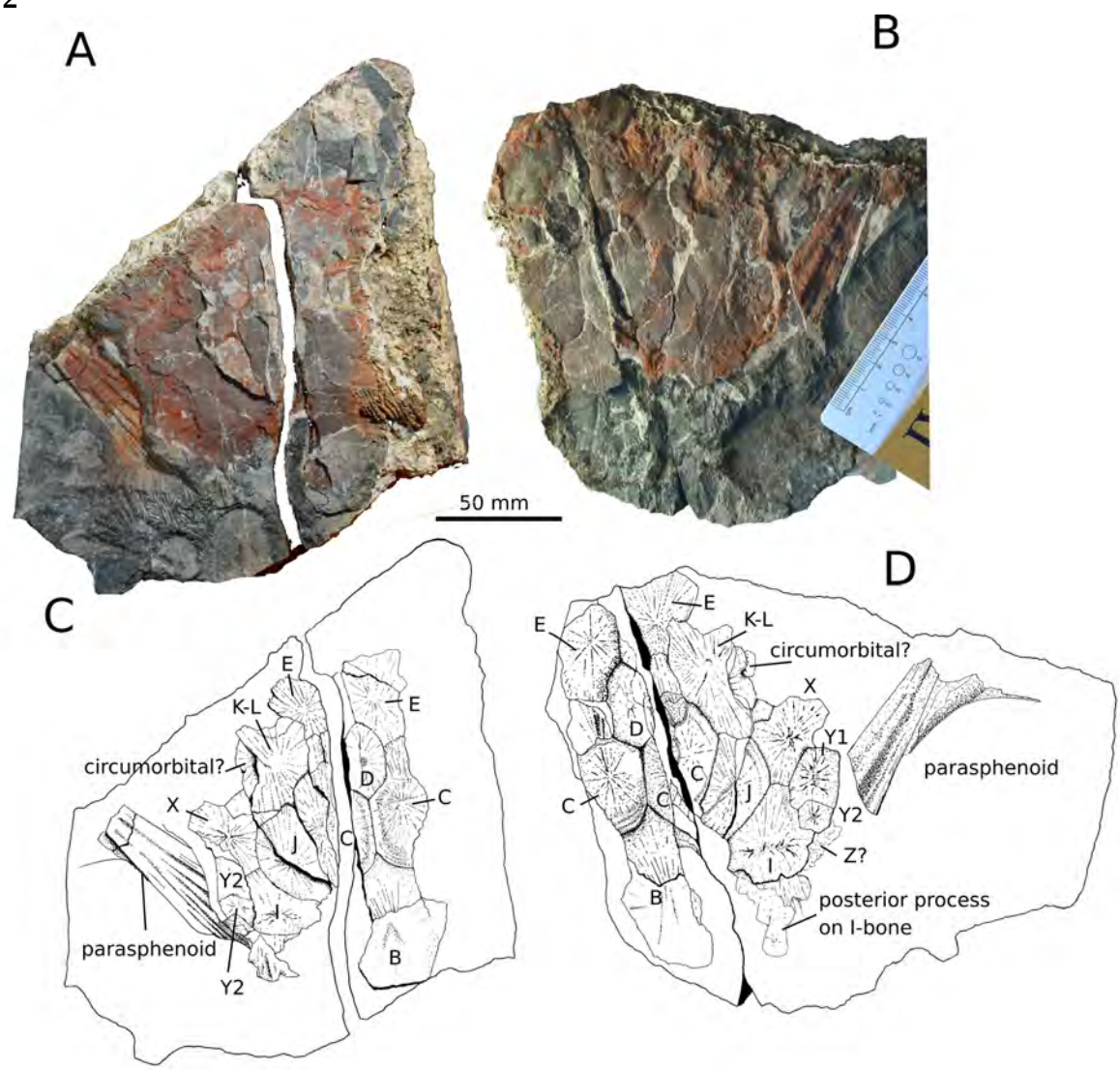

Figure 3

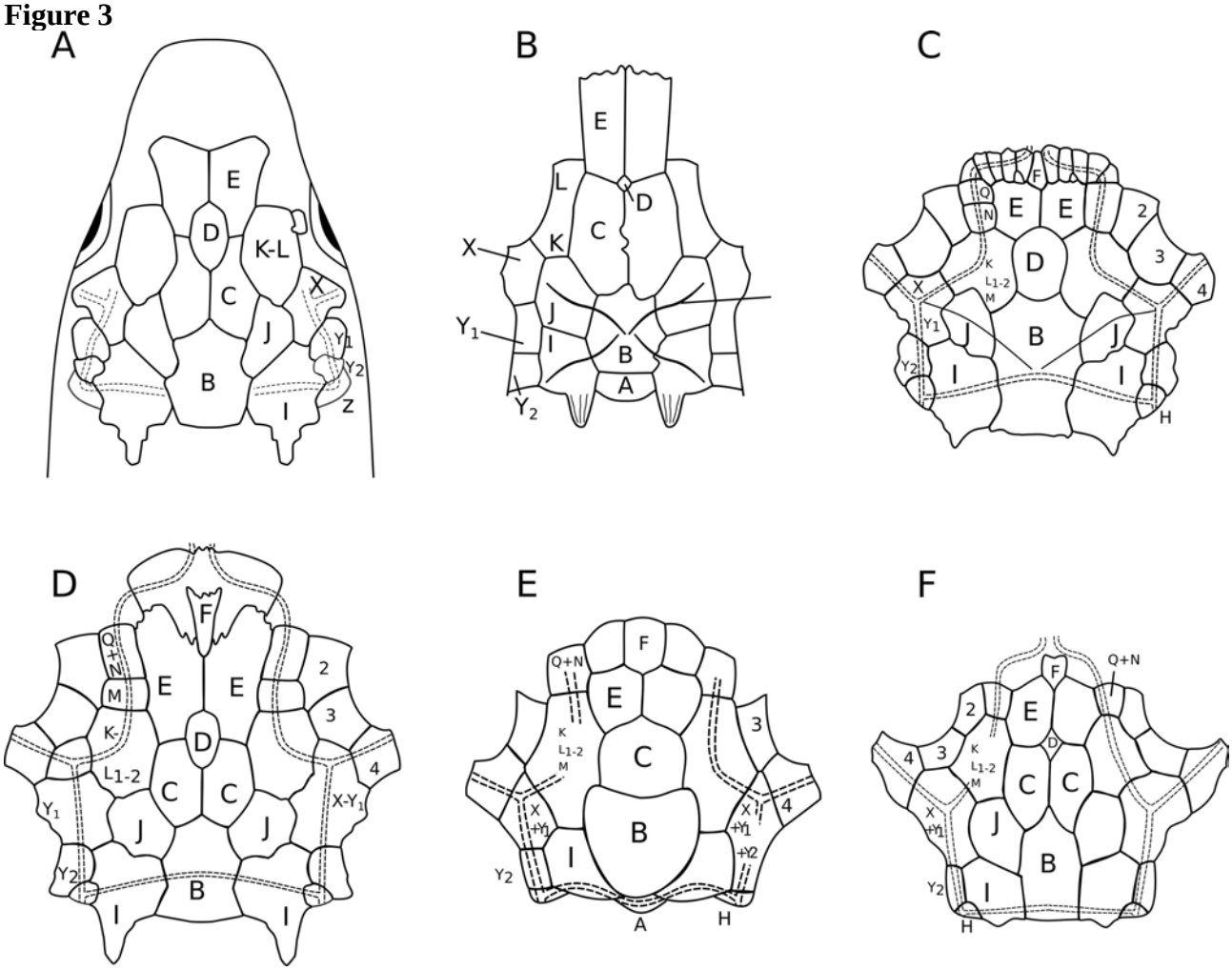

Figure 4

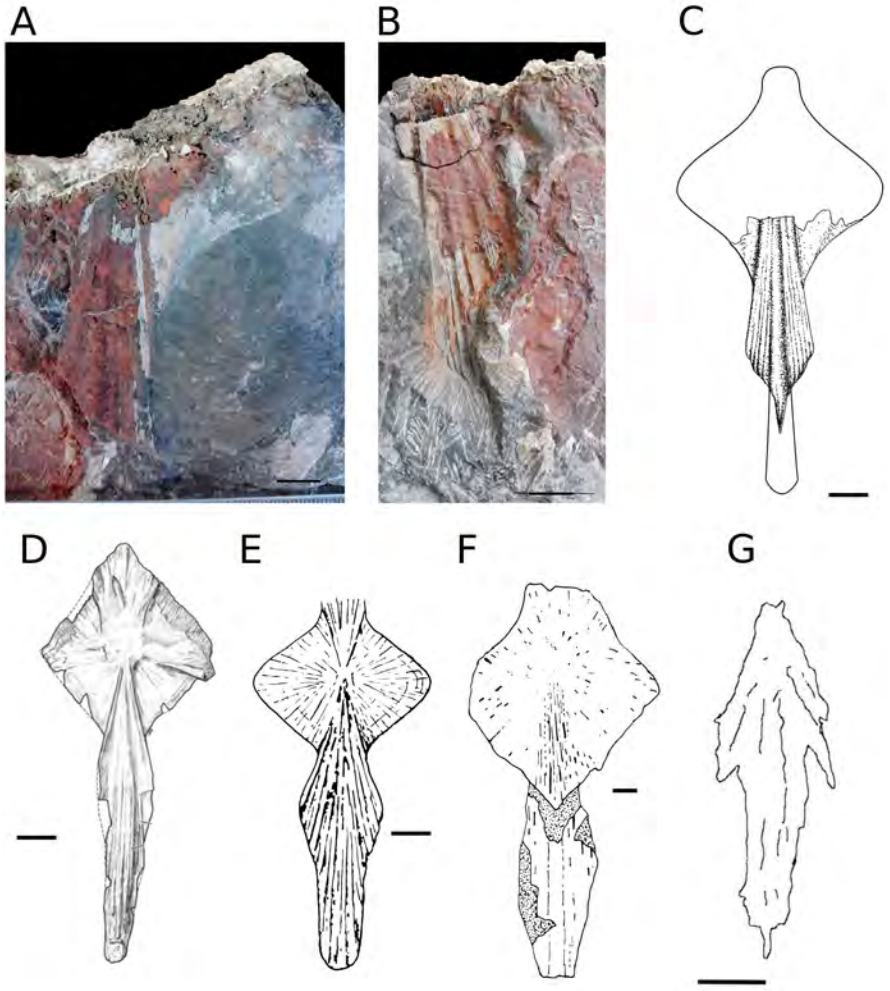

Figure 5

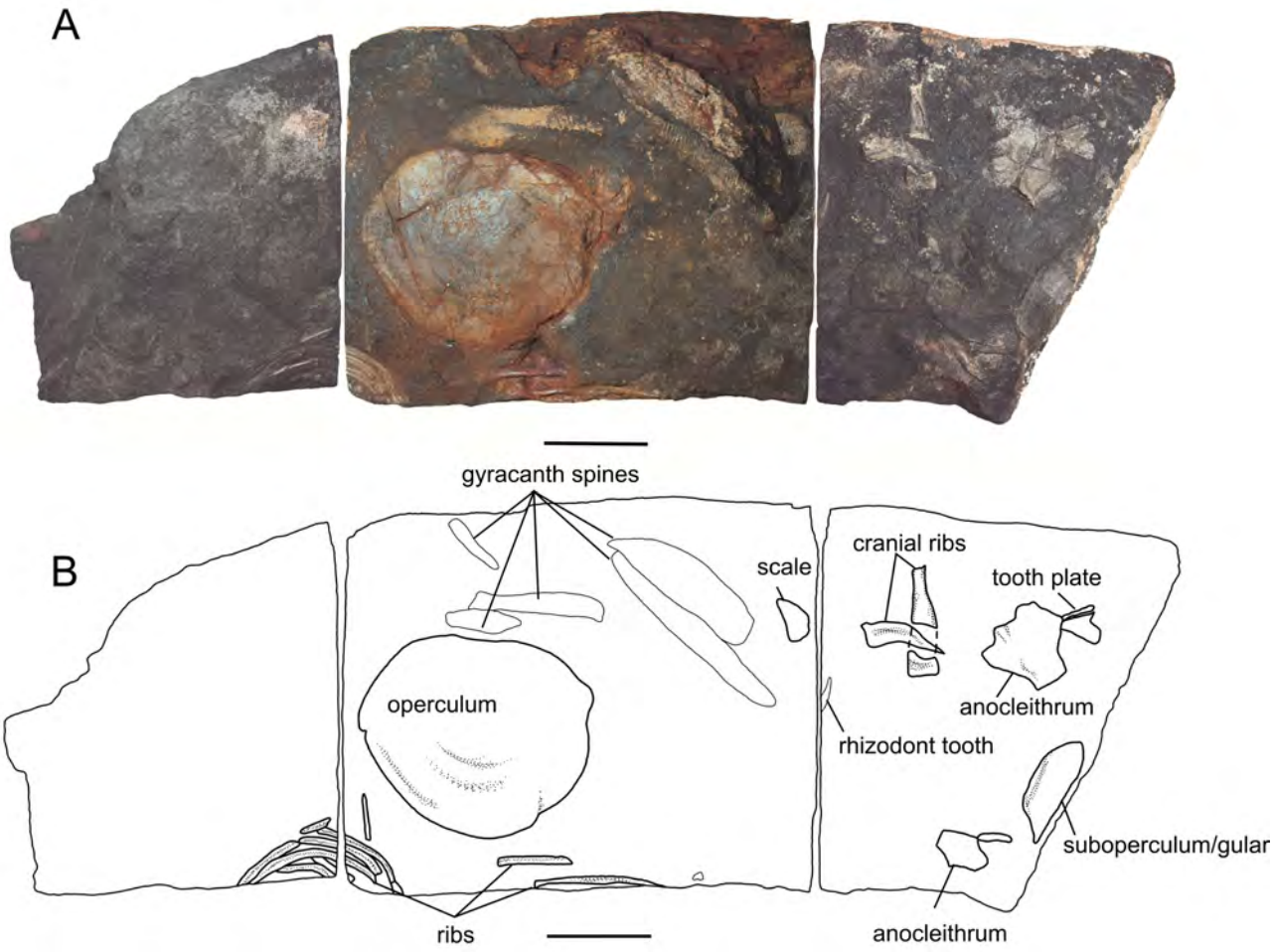

Figure 6

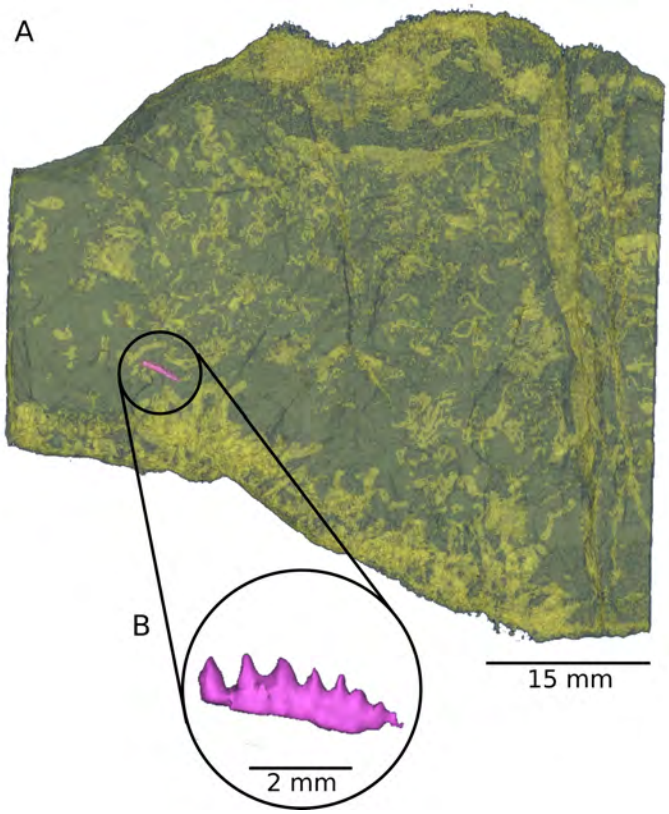

Figure 7

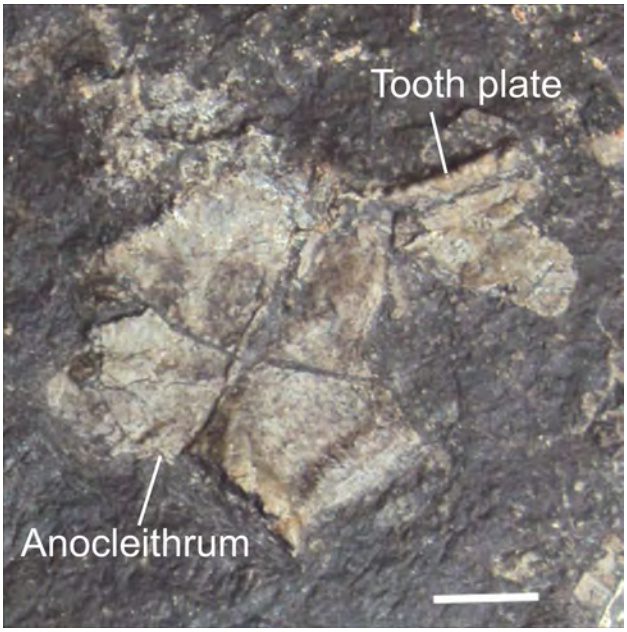

Figure 8

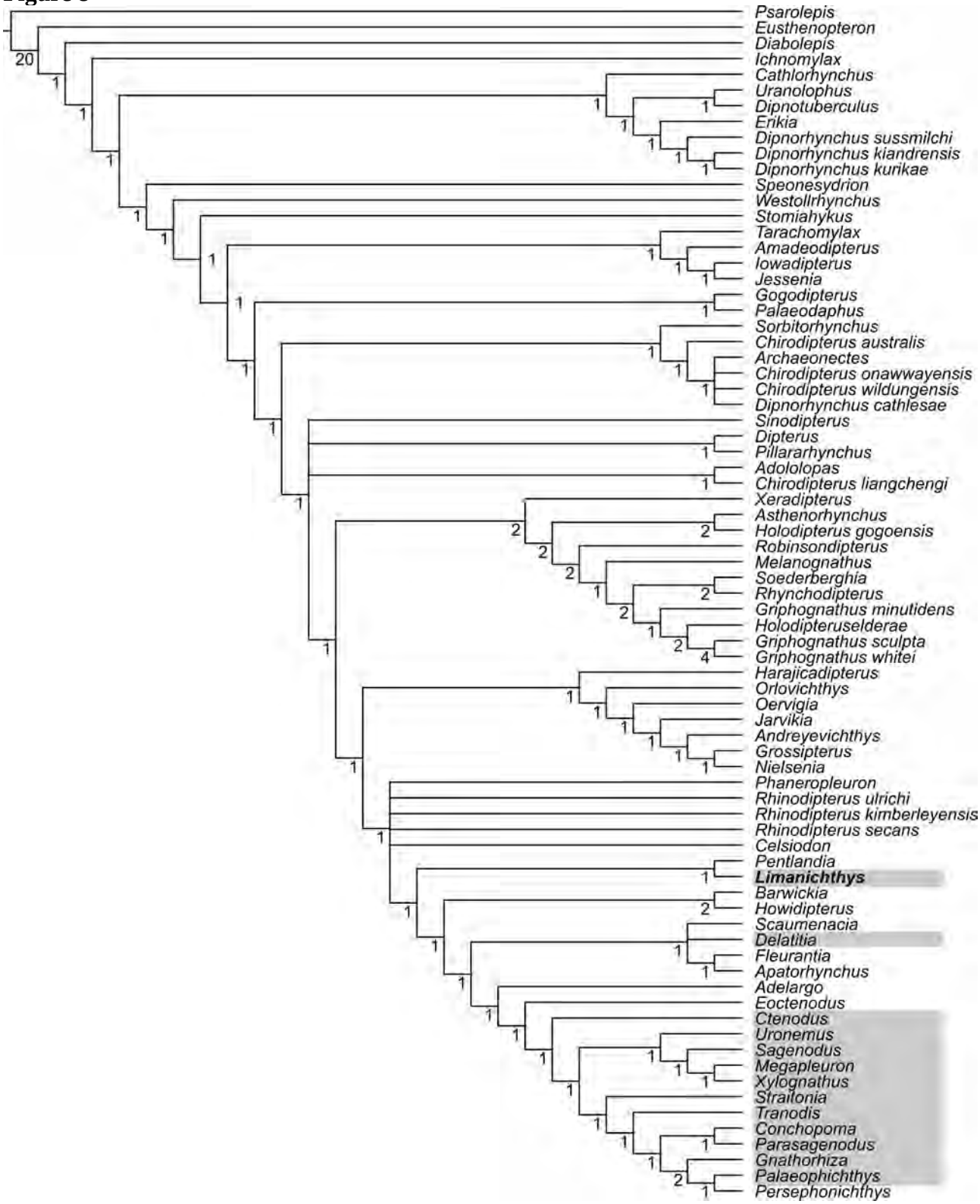
Psarolepis
Eusthenopteron
Diabolepis
Ichnomylax
Cathlorhynchus
Uranolophus
Dipnotuberculus
Erikia
Dipnorhynchus sussmilchi
Dipnorhynchus kiandrensis
Dipnorhynchus kurikae
Speonesydrion
Westollrhynchus
Stomiahykus
Tarachomylax
Amadeodipterus
Iowadipterus
Jessenia
Gogodipterus
Palaeodaphus
Sorbitorhynchus
Chirodipterus australis
Archaeonectes
Chirodipterus onawwayensis
Chirodipterus wildungensis
Dipnorhynchus cathlesae
Sinodipterus
Dipterus
Pillararhynchus
Adololopas
Chirodipterus liangchengi
Xeradipterus
Asthenorhynchus
Holodipterus gogoensis
Robinsondipterus
Melanognathus
Soederberghia
Rhynchodipterus
Griphognathus minutidens
Holodipteruselderae
Griphognathus sculpta
Griphognathus whitei
Harajicadipterus
Orlovichthys
Oervigia
Jarvikia
Andreyevichthys
Grossipterus
Nielsenia
Phaneropleuron
Rhinodipterus ulrichi
Rhinodipterus kimberleyensis
Rhinodipterus secans
Celsiodon
Pentlandia
Limanichthys
Barwickia
Howidipterus
Scaumenacia
Delatitia
Fleurantia
Apatorhynchus
Adelargo
Eoctenodus
Ctenodus
Uronemus
Sagenodus
Megapleuron
Xylognathus
Strailonia
Tranodis
Conchopoma
Parasagenodus
Gnathorhiza
Palaeophichthys
Persephonichthys

Figure 9

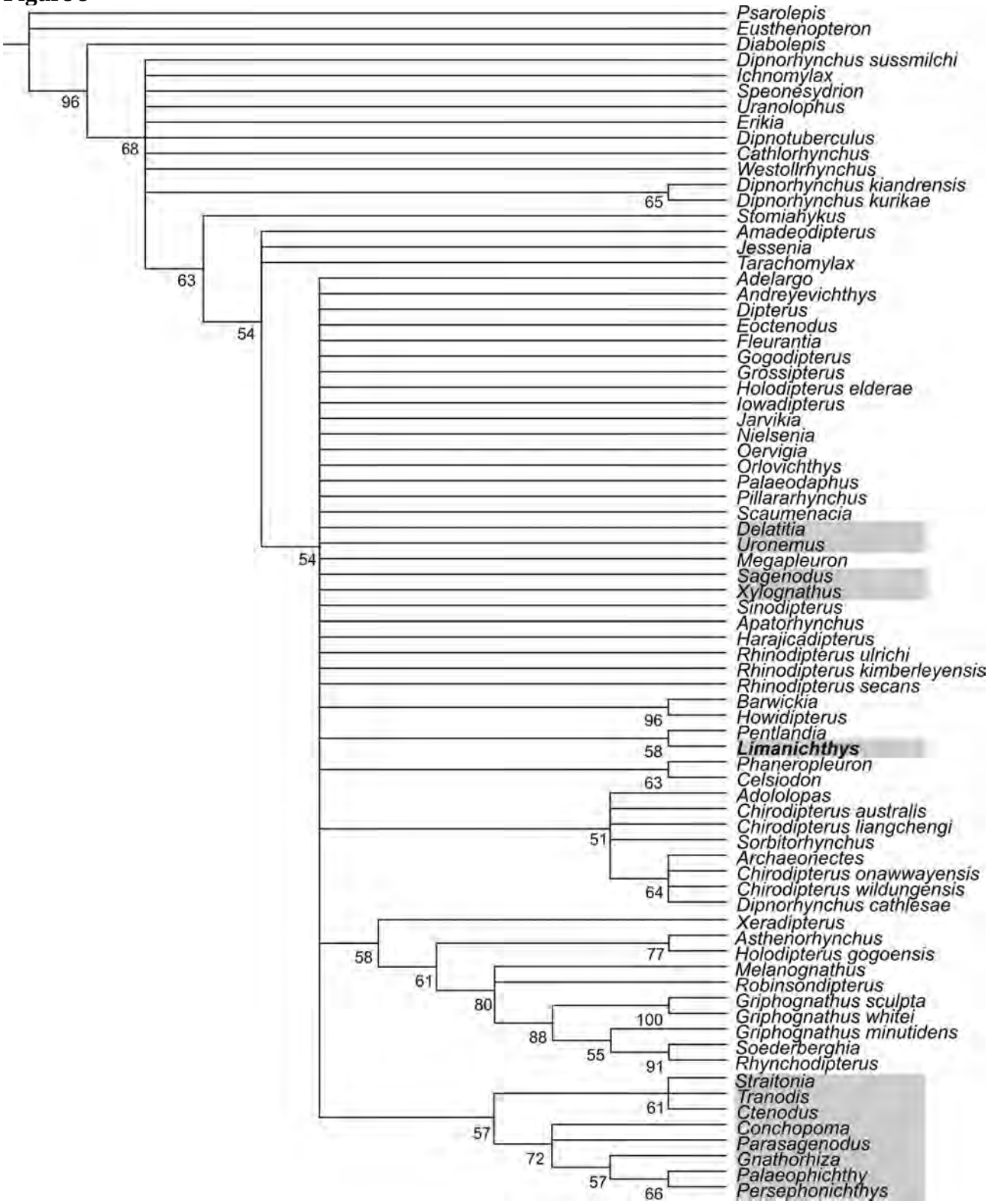
Psarolepis
Eusthenopteron
Diabolepis
Dipnorhynchus sussmilchi
Ichnomylax
Speonesydrion
Uranolophus
Erikia
Dipnotuberculus
Cathlorhynchus
Westollrhynchus
Dipnorhynchus kiandrensis
Dipnorhynchus kurikae
Stomiahykus
Amadeodipterus
Jessenia
Tarachomylax
Adelargo
Andreyevichthys
Dipterus
Eoctenodus
Fleurantia
Gogodipterus
Grossipterus
Holodipterus elderae
Iowadipterus
Jarvikia
Nielsenia
Oervigia
Orlovichthys
Palaeodaphus
Pillararhynchus
Scaumenacia
Delatitia
Uronemus
Megapleuron
Sagenodus
Xylognathus
Sinodipterus
Apatorhynchus
Harajicadipterus
Rhinodipterus ulrichi
Rhinodipterus kimberleyensis
Rhinodipterus secans
Barwickia
Howidipterus
Pentlandia
Limanichthys
Phaneropleuron
Celsiodon
Adololopas
Chirodipterus australis
Chirodipterus liangchengi
Sorbitorhynchus
Archaeonectes
Chirodipterus onawwayensis
Chirodipterus wildungensis
Dipnorhynchus cathlesae
Xeradipterus
Asthenorhynchus
Holodipterus gogoensis
Melanognathus
Robinsondipterus
Griphognathus sculpta
Griphognathus whitei
Griphognathus minutidens
Soederberghia
Rhynchodipterus
Straitonia
Tranodis
Ctenodus
Conchopoma
Parasagenodus
Gnathorhiza
Palaeophichthy
Persephonichthys
96
68
65
63
54
54
96
58
63
51
64
58
77
61
80
100
88
55
91
61
57
72
57
66

Figure 10

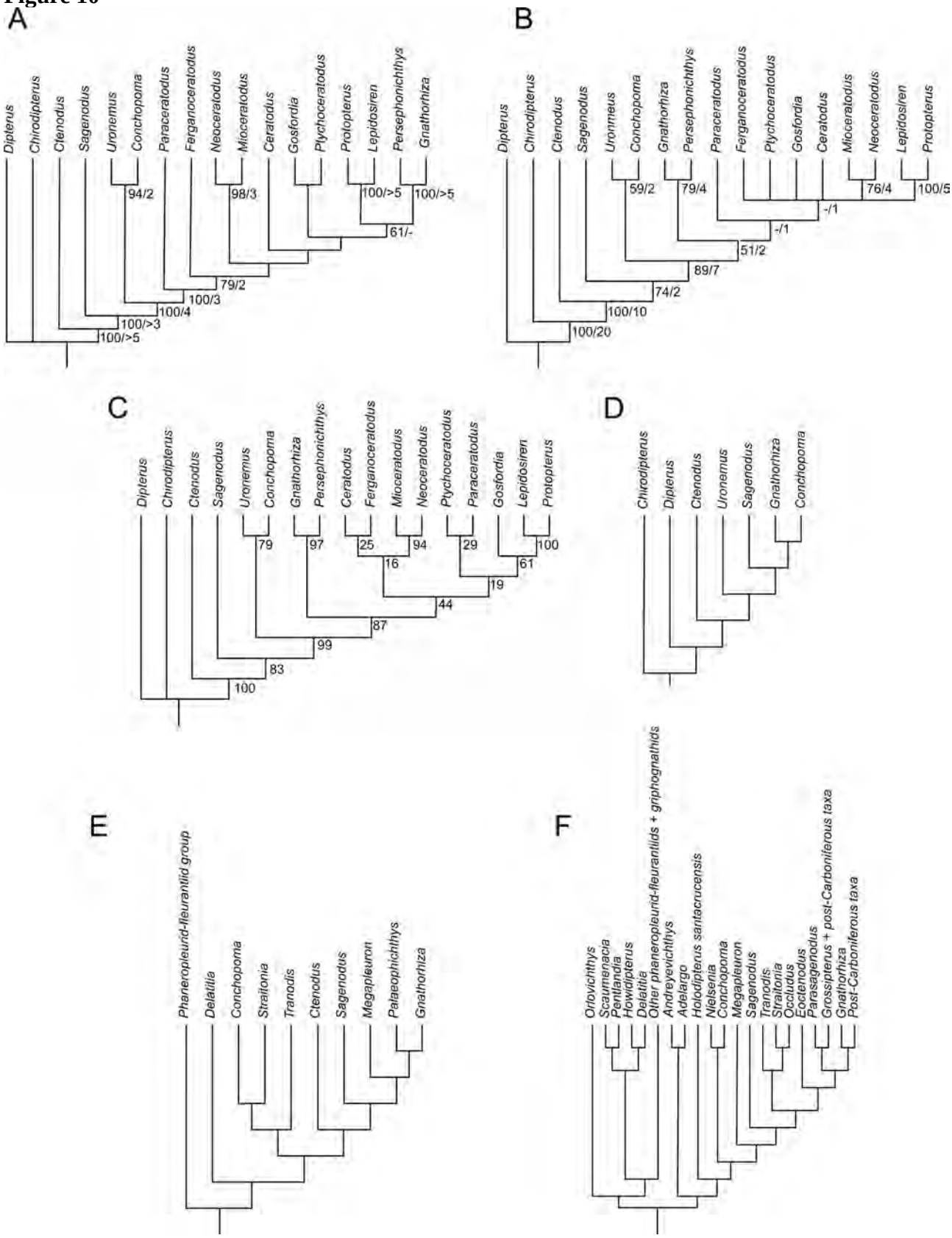
A
Dipterus
Chirodipterus
Ctenodus
Sagenodus
Uronemus
Conchopoma
Paraceratodus
Ferganoceratodus
Neoceratodus
Miloceratodus
Ceratodus
Gosfordia
Ptychoceratodus
Protopterus
Lepidosiren
Persephonichthys
Gnathorhiza
94/2
98/3
100/>5
100/>5
61/-
79/2
100/3
100/4
100/>3
100/>5
B
Dipterus
Chirodipterus
Ctenodus
Sagenodus
Uronmeus
Conchopoma
Gnathorhiza
Persephonichthys
Paraceratodus
Ferganoceratodus
Ptychoceratodus
Gosfordia
Ceratodus
Miloceratodus
Neoceratodus
Lepidosiren
Protopterus
59/2
79/4
76/4
100/5
-/1
-/1
51/2
89/7
74/2
100/10
100/20
C
Dipterus
Chirodipterus
Ctenodus
Sagenodus
Uronemus
Conchopoma
Gnathorhiza
Persephonichthys
Ceratodus
Ferganoceratodus
Miloceratodus
Neoceratodus
Ptychoceratodus
Paraceratodus
Gosfordia
Lepidosiren
Protopterus
79
97
25
94
29
100
61
16
19
44
87
99
83
100
D
Chirodipterus
Dipterus
Ctenodus
Uronemus
Sagenodus
Gnathorhiza
Conchopoma
E
Phaneropleurid-fleurantiid group
Delatitia
Conchopoma
Straitonia
Tranodis
Ctenodus
Sagenodus
Megapleuron
Palaeophichthys
Gnathorhiza
F
Orlovichthys
Scaumenacia
Pentlandia
Howidipterus
Delatitia
Other phaneropleurid-fleurantiids + griphognathids
Andreyevichthys
Adelargo
Holodipterus santacrucensis
Nielsenia
Conchopoma
Megapleuron
Sagenodus
Tranodis
Straitonia
Occludus
Eoctenodus
Parasagenodus
Grossipterus + post-Carboniferous taxa
Gnathorhiza
Post-Carboniferous taxa

CHARACTER LIST

All characters are from Clack *et al*. (*in review*) which are derived from Qiao & Zhu (2015), Qiao & Zhu (2009), Schultze (2001), Ahlberg *et al*. (2006) and Friedman (2007) with modifications as-described below.

1. Pineal opening: 0. open; 1. closed. Schultze and Marshall (1993; char. 1), Schultze (2001; char. 1), Ahlberg et al, (2006; char. 55), Qiao and Zhu (2009; char. 1).

2. Pineal region marked by short eminence: 0. no; 1. yes.

3. Cosmine present on skull: 0. yes, full cover; 1. yes, but strongly reduced; 2. no. (ordered)

4. Length of B bone: 0. short (less than 2 times its width); 1. long (equal or more than 2 times its width); 2. broad (wider than long).

5. Pit-lines on B bone: 0. absent; 1. anterior and middle pit-line present; 2.only anterior pit-line.

6. C bone: 0. absent; 1. present.

7. D-bone: 0. many; 1. single; 2. absent.

8. Contact between E and C bones: 0. absent; 1. present.

9. Paired E bones: 0. mosaic; 1 present; 2. single E-bone; 3. absent The polarity of this character has been reversed from 0. absent; 1. present; 2. mosaic to reflect the occurrence of this character in the oldest (most basal) to more recent (derived) dipnoan taxa.

10. Length of E-bone(s): 0. less than twice their width; 1. more than twice their width.

11. I-bones meeting in midline: 0. yes; 1. no, separated by B bone. This character changed to just refer to I-bones rather than implying homology between the I-bones and postparietals.

12. Posterior process of I bone: 0. absent; 1. present.

13. J-bones meeting in midline: 0. yes; 1. no. This character changed to just refer to J-bones rather than implying homology between the J-bones and parietals.

14. L-bone: 0 = two present, 1 = one present, 2 = fused K+L, 3 = fused K+L+M, 4 = other bones included. Schultze and Marshall (1993; char. 25), Schultze and Chorn (1997; char. 10,37,38,39,40), Schultze (2001; char. 25), Schultze (2004; char. 18).

15. Length of L-bone: 0. similar to others in supraorbital canal series; 1. about twice as long as others in supraorbital canal series.

16. K-bone: 0 = single, 1 = space of K+X, 2 = neither single nor K+X (e.g. fused (i.e 'space of') K- + L-bones) , 3 = K-bone absent. Schultze and Marshall (1993; char. 24), Schultze and Chorn (1997; char. 9,36), Schultze (2001; char. 24), Schultze (2004; char. 17).

17. K bone: 0. medial to X bone; 1. anterior to X bone; 2. in sequence.

18. M bone: 0. present; 1. absent.

19. N bone: 0. present; 1. absent.

20. Q bone: 0. absent; 1. present.

21. Z bone: 0. posterior to I bone; 1. lateral to I bone.

22. Maximum width of skull roof situated posterior to the level of the bone Y_1: 0. yes; 1. No.

23. Sutures between median series of skull roofing bones: 0 = straight, 1 = interdigitate, 2 = open. Schultze and Marshall (1993; char. 3), Schultze (2001; char. 3), Schultze (2004; char. 1).

24. Elongated snout: 0. absent; 1. present.

25. Ossified upper lip in adult: 0. mosaic; 1. fused; 2. absent.

26. Snout/skull roof: 0. with diffuse posterior margin; 1. with sharp posterior margin. (Uncertain for *Eusthenopteron* but coded as '1' given the clear demarcation between naso-parietal-frontal? and parietals).

27. Supraorbital and infraorbital canals: 0. separated; 1. connected.

28. Lateral line in bone 3: 0. absent; 1. present.

29. Cheek bones: 0. cheek bones 1-11 present; 1. no 11; 2. no 10, 11.

30. Length of postorbital cheek: 0. substantially longer than diameter of orbit; 1. equal to or shorter than diameter of orbit.

31. Ratio length snout:cheek: 0. <1; 1. >=1. (Schultze & Marshal (1993) definition: Ratio snout/cheek: 0 = 1:1, 1 = 2 (>1.5):1, 2 = 3 (>2.5):1, 3 = >4:1. Schultze and Marshall (1993;

char. 85), Schultze (2001; char. 85), Schultze (2004; char. 53).)

32. Bone 6: 0. reaching ventral margin of cheek; 1. excluded from ventral margin of cheek by bone 10.

33. Bone 7: 0. approximately equilateral; 1. much longer than deep.

34. Size of bone 10 (quadratojugal): 0. large, as 5 or greater; 1. much smaller than 5, or absent.

35. Subopercular: 0. two; 1. one.

36. Buccohypophyseal opening (foramen): 0. present; 1. absent.

37. Palatal construction: 0. parasphenoid separates pterygoids; 1. pterygoids articulate with each other with suture; 2. pterygoids fused.

38. Parasphenoid: 0. fused into palate; 1. visible sutures; 2. overlapping (pterygoids).

39. Transverse curvature of palate: 0. flat; 1. arched.

40. Parasphenoid stalk: 0. no stalk; 1. simple stalk without sharp division into tapering proximal portion and parallel-sided distal portion; 2. stalk with sharp division into tapering proximal portion and parallel-sided distal portion. (ordered)

41. Ratio of posterior length to anterior length of parasphenoid: 0. less than 1 or about 1; 1. greater than 1.

42. Furrow on ventral surface of parasphenoid stalk: 0. absent; 1. present.

43. Furrow on dorsal surface of parasphenoid stalk: 0. absent; 1. present.

44. Parasphenoid bearing denticle-lined ascending process: 0. no; 1. yes.

45. Dental material on parasphenoid: 0. present; 1. absent.

46. Parasphenoid reaching posterior margin of occiput: 0. no; 1. yes.

47. Shape of parasphenoid: 0 = anteriad elongated, 1 = plow-shaped, 2 = with lozenge, 3 = round anterior portion, 4 = angled anterior portion. Schultze and Marshall (1993; char. 49), Schultze and Chorn (1997; char. 18), Schultze (2001; char. 49), Schultze (2004; char. 34).

48. Position of parasphenoid: 0. below ethmosphenoid; 1. below otico-occipital; 2. below both.

49. Position of anterior end of parasphenoid: 0. in front of jaw articulation; 1. not in front.

50. Ratio of maximum width of parasphenoid to distance of articulation points of jaws: 0. less than 1/3; 1. between 1/3 and 2/3; 2. greater than 2/3.

51. Lateral angle of parasphenoid: 0 = no angle, 1 = angular, 2 = rounded, 3 = reflexed. Schultze and Marshall (1993; char. 48), Schultze (2001; char. 48), Schultze (2004; char. 33).

52. (Posterior) end of parasphenoid (stalk): 0. single point; 1. bifid; 2. trifid with lateral projections.

53. Margins of posterior stalk of parasphenoid: 0. converge to posterior angle; 1. subparallel.

54. “Vomer” *sensu* Miles (1977): 0. present; 1. absent.

55. “Dermopalatine 1” *sensu* Miles (1977): 0. median; 1. paired.

56. “Dermopalatine 1” *sensu* Miles (1977) / pterygoid: 0. fused to pterygoid; 1. present, not in contact; 2. isolated.

57. Series anterolateral to pterygoids: 0. present, with tusks; 1. present with denticles or dentine sheet; 2. present with tooth row. This is interepreted as meaning ‘dental’ series anterolateral to pterygoids.

58. Parasphenoid separating pterygoids along more than half of their length: 0. yes; 1. no.

59. Angle between midline and anterolateral margin of pterygoid: 0. less than 55 degrees; 1. more than 55 degrees. From Ahlberg et al (2006), character 24 and Qiao & Zhu (2009; 2015).

60. Anterior nostril: 0. located dorsal to oral margin; 1. marginal.

61. Posterior nostril: 0. located dorsal to oral margin; 1. marginal 2. palatal. (ordered)

62. Internasal pits: 0. well developed; 1. reduced or absent.

63. Cosmine-like tissue within oral cavity: 0. no; 1. yes.

64. Premaxilla: 0. present; 1. absent.

65. Lateral lines in mandible: 0. parallel; 1. converging in one bone. *Diplocercides* only has one

lateral line canal in the mandible (Forey et al, 2000).

66. Length of symphysis (ratio length of symphysis to length of jaw): 0. greater than 1/3; 1. between 1/5 and 1/3; 2. less than 1/5.

67. Adsymphysial plate: 0 = present, but fused, 1 = isolated, sutured bone, 2 = missing. Schultze and Marshall (1993; char. 66), Schultze (2001; char. 66), Schultze (2004; char. 45).

68. “Dentary”: 0. unpaired ; 1. paired; 2. absent.

69. Dentary-prearticular relationship: 0. dentition-generating gap; 1. small midline hole only ; 2. no gap.

70. Slot between dentary and prearticular: 0. broad; 1. narrow; 2. no slot.

71. Adductor fossa: 0. not overhung by prearticular; 1. overhung by prearticular.

72. Length of adductor fossa: 0. more than 20% of jaw length; 1. 5%-20% of jaw length; 2. 0-5% of jaw length (ordered). For *Diplocercides*, see Friedman (2007) fig. 5c.

73. Morphology of adductor fossa: 0. open; 1. reduced to vestigial slit.

74. Coronoids: 0. present; 1. absent.

75. Lip fold: 0. absent; 1. present.

76. Meckelian bone: 0. wholly ossified; 1. only articular ossified, or not ossified at all.

77. Retroarticular process: 0. small and poorly developed; 1. robust, squarish.

78. Skin contact surface on infradentary bones: 0. reaching up to lip of adductor fossa; 1. widely separated from lip of adductor fossa. 1

79. Curvature of ventral mandibular margin: 0. strongly convex; 1. essentially flat.

80. Orientation of glenoid: 0. mostly dorsally; 1. posterodorsally.

81. Shape of glenoid fossa: 0. double structure; 1. single groove.

82. Angular and surangular: 0. separate; 1. fused into a single long bone.

83. Splenial and postsplenial: 0. separate; 1. fused. For *Diplocercides*, coded as '?' due to uncertainty of homology and from fusion of infradentaries (see Friedman, 2007).

84. Teeth on upper lip: 0. shedding teeth; 1. statodont tooth row; 2. teeth absent.

85. Teeth on dentary: 0. shedding teeth present; 1. statodont tooth rows present; 2. teeth absent.

86. Number of tooth ridges *in adult specimens*: 0. <10; 1. >10. Kemp (1977) clearly demonstrated that the number of tooth ridges in growing *Neoceratodus forsteri* increases from larval stage to adult and that the number of tooth ridges differs between the lower and upper jaws. When coding for this character it is important to account for the complete growth series of the taxon and if this is not possible, justification must be given for coding for this character.

87. Tooth plates: 0. present; 1. absent. Not applicable in thte context of outgroup otherwise absence would be considered a reversal.

88. Morphology of teeth on pterygoid and prearticular: 0. round/conical; 1., forming distinct proximodistal cutting ridge.

89. Addition of large dentine elements at regular intervals to lateral margin of pterygoid/ prearticular: 0. yes; 1. no.

90. Nature of large dentine elements: 0. teeth; 1. petrodentine cores; 2. thick irregular dentine; 3. ridges narrow regular dentine ridges.

91. Addition of marginal blisters to pterygoid/prearticular: 0. no; 1. yes.

92. Shape of marginal blisters: 0. bead-shaped; 1. elongated strips.

93. Addition of inter-row dentine along edge of pterygoid/ prearticular: 0. no; 1. yes.

94. Nature of inter-row dentine: 0. always fuses or wears down into sheet; 1. separate denticles persist between some tooth rows.

95. Pulp cavity: 0. tooth plates without pulp cavity; 1. with pulp cavity.

96. Diffuse dentine deposition on surface of palate/lower jaw: 0. yes, diffusely across whole palate; 1. no; 2. redeposition of denticles only within “footprint” (outer circumference) of resorbed tooth plate.

97. Relative areas of denticle field/thin dentine sheet on palate: 0. all or nearly all denticles; 1. both dentine sheet and denticles; 2. mostly dentine sheet; 3. denticles outside toothplate; 4 dentine sheet on resorption areas within toothplate.

98. Relative areas of denticle field and dentine sheet on lower jaw: 0. all or nearly all denticles; 1. both denticles and dentine sheet; 2. mostly dentine sheet.

99. Resorption of dentition on pterygoid/prearticular plate origin: 0. little or no resorption, origin left unmodified; 1. extensive resorption, removing mesial parts of plate; 2. resorption and deposition of dentine sheet within toothplate only, not crossing edges.

100. Distinct vertically growing “heel” on prearticular: 0. no; 1. yes.

101. Petrodentine: 0. absent; 1. present.

102. Sharp “additive” mesial and posterior edges on tooth plates: 0. absent; 1. present.

103. Behaviour of “additive edges” (if present): 0. quiescent; 1. active.

104.Braincase/skull table relationship: 0. broad contact; 1. supported by cristae.

105. Angle between quadrate and plane of parasphenoid: 0. 90-95 degrees; 1. 80 -65 degrees; 2. 55-35 degrees.

106. Autostyly: 0. absent; 1. present.

107. Lateral commissure: 0. separate from palatoquadrate; 1. partly fused but distinguishable; 2.

wholly fused to palatoquadrate. (ordered). The presence of a structure termed the lateral commissure in Dipnoi was rejected by Miles (1977).

108. Palatoquadrate: 0. fused into palate; 1. free.

109. Dorsolateral process on palatoquadrate: 0. absent; 1. present.

110. Metotic (lateral otic) fissure: 0. present; 1. absent.

111. Intracranial joint/ventral cranial fissure: 0. mobile joint; 1. ventral cranial fissure; 2. neither fissure nor joint.

112. Occiput inset from posterior margin of neurocranium: 0. no; 1. yes.

113. Notochordal canal occluded by ossified cranial centrum: 0. no; 1. yes.

114. Neural cavity and notochordal canal separated by an ossified shelf in the occipital region, posterior to the foramen for N. X: 0. yes; 1. no.

115. Ossification complete along ventral midline of notochordal canal posteriorly: 0. yes; 1. no.

116. Occipital region bears transverse processes flanking foramen magnum: 0. no; 1. yes.

117. Dorsal aorta: 0. divides at or anterior to occiput; 1. divides posterior to occiput. (Friedman, 9).

118. Lateral dorsal aortae: 0. run along ventral surface of neurocranium; 1. run in grooves on parasphenoid.

119. Occipital artery extramural: 0. no; 1. yes.

120. Neurocranium extends far posterior to hind margin of postparietals: 0. no; 1. yes.

121. Dorsolateral crista fenestrated: 0. no; 1. yes.

122. Median crista discontinuous: 0. no; 1. yes.

123. Little or no overlap between intersections of median and dorsolateral cristae with the dermal skull roof (median crista abbreviated): 0. no; 1. yes.

124. Lateral cristae fenestrated: 0. no; 1. yes.

125. Development of a pronounced ridge anterior to and continuous with the dorsolateral cristae: 0. no; 1. yes.

126. Articulation of first epibranchial posterior to the level of the foramen for N. IX: 0. no; 1. yes.

127. Notochord extending to or beyond level of N. V: 0. yes; 1. no.

128. Development of a deep “spiracular recess” *sensu* Thomson and Campbell (1971): 0. yes; 1. no.

129. Separate foramina for the internal carotid artery and efferent pseudobranchial artery: 0. no; 1. yes.

130. Jugular vein: 0. little or no groove; 1. travels through deep groove along length of otic region.

131. Foramina for the jugular vein and the ramus hyomandibularis N. VII on the posterior surface of the transverse wall of the otic region: 0. confluent; 1. separate.

132. Foramina for the jugular vein and the orbital artery on the posterior surface of the transverse wall of the otic region: 0. confluent; 1. separate.

133. Foramina for the ramus hyomandibularis N. VII and the orbital artery on the posterior surface of the transverse wall of the otic region: 0. confluent1; 1. separate.

134. Hyomandibular facet traverses fissure in transverse otic wall (hyomandibular facet extends on to palatoquadrate): 0. no; 1. yes.

135. Separate ossified canals for pineal and parapineal organs: 0. yes; 1. no.

136. Foramen for N. II above the level of foramen sphenoticum minus: 0. no; 1. yes.

137. Foramen for N. III above level of foramen sphenoticum minus: 0. no; 1. yes.

138. Ventral face of nasal capsule: 0. complete; 1. perforated by fenestration that opens posteroventrolaterally (fenestra ventralis); 2. solum nasi completely unossified. (ordered).

139. Nasal capsule set well posterior to snout margin or preoral eminence: 0. no; 1. yes.

140. Enlarged, knob-shaped protrusion on the posteroventral surface of the quadrate (hyosuspensory eminence of Miles, 1977): 0. absent; 1. present.

141. Overlap relationship between entopterygoids and parasphenoid: 0. parasphenoid overlaps entopterygoids dorsally; 1. entopterygoids overlap parasphenoid dorsally.

142. Cleithrum and clavicle: 0. with cosmine; 1. without cosmine.

143. Median fin morphologies: 0. all separate and short-based; 1. posterior dorsal fin long-based; 2. both dorsal fins long-based uninterrupted fin fringe.

144. Posterior dorsal fin support: 0. all radials carried by basal plate; 1. anterior radials on basal plate, posterior radials free; 2. no basal plate.

145. Anal fin support: 0. trapezoidal with no distinct shaft; 1. cylindrical proximal shaft and triangular distal plate.

146. Median fin radials: 0. cylindrical; 1. hourglass-shaped.

147. Vertebral column: 0. unconstricted notochord; 1. disc centra.

148. Neural arches and spines: 0. separate; 1. fused.

149. Scales: 0. rhombic; 1. round.

150. Cosmine on scales: 0. present; 1. absent.

151: Adlateral cristae (postero-dorsal extensions of the lateral cristae that connect the otic region of the neurocranium to the visceral surface of the dermal skull roof) present: 0. yes; 1. no.

(Character 15 in Friedman 2007)

152: Median callus on palate: 0. absent; 1. present. (Character 18 in Ahlberg *et al*. 2006)

153: B bone: 0. absent; 1. present. (Character 8 in Schultze, 2001).

154: Foramen for the internal carotid anterior to that for the efferent pseudobranchial artery: 0. no; 1. yes. (Character 29 in Friedman 2007)

155. Ossification of neurocranium: 0 - completely ossified; 1 – poorly-ossified/cartilagenous.

156 = Character 11 of Lloyd *et al*. (2012). C-bone(s): 0 – paired; 1 – single. Character state '1' changed from '*single/absent*' to differentiate between character 6: C-bone: 0. absent; 1. absent.

157. Angle between first and last tooth ridge: 0 - 50 – 100°; 1- less than 50° or greater than 100$^{o.}$

158. Character 62 of Lloyd *et al*. (2012). Lower jaw: 0 = short mandible rami, 1 = elongated rami with short symphysis, 2 = elongated symphysis. Schultze and Marshall (1993; char. 61), Schultze (2001; char. 61).

159. Character 4 of Lloyd *et al*. (2012). Kinesis between nasal region and braincase behind it: 0 = absent, 1 = present. Schultze and Marshall (1993; char. 4), Schultze (2001; char. 4), Schultze (2004; char. 2).

160. Character 5 of Lloyd *et al*. (2012). A-bone: 0 = independent A-bone, 1 = not present as independent bone, 2 = incorporated into skull roof. Schultze and Marshall (1993; char. 5), Schultze (2001; char. 5), Schultze (2004; char. 3).

161. Character 6 of Lloyd *et al*. (2012). Supraoccipital commissure: 0 = through Z-G-I-A-I-G-Z, 1 = through I-A-I, 2 = through I-B-I, 3 = through Z-B-Z, 4 = above bones. Schultze and 1Marshall (1993; char. 6), Schultze and Chorn (1997; char. 3), Schultze (2001; char. 6), Schultze (2004; char. 4).

162. Character 10 of Lloyd *et al*. (2012). Adductor muscles: 0 = below skull roof, 1 = above skull roof. Schultze and Marshall (1993; char. 10), Schultze (2001; char. 10), Schultze (2004; char. 8).

163. Character 15 of Lloyd *et al*. (2012). F-bone: 0 = not existing, 1 = present, 2 = place of F+E. Schultze and Marshall (1993; char. 15), Schultze (2001; char. 15), Schultze (2004; char. 12).

164. Character 16 of Lloyd *et al*. (2012). Space taken by K+L or more bones (i.e. K- and L-bones missing if '0'): 0 = not, 1 = yes, 2 = in addition M, 3 = in addition M+N, 4 = in addition J+M, 5 = in addition X. Schultze and Marshall (1993; char. 16), Schultze (2001; char. 16), Schultze (2004; char. 13).

165. Character 18 of Lloyd *et al*. (2012). G-bone: 0 = present, 1 = absent. Schultze and Marshall (1993; char. 18), Schultze (2001; char. 18). This character is logically possible for taxa outside the in group though in considering so the polarity is confused. Schultze and Marshall (1993) do not test the polarity of the character with the context of an outgroup and so we code it as '?' for non-dipnoan taxa in this study.

166. Character 19 of Lloyd *et al*. (2012). I-bone: 0 = present, 1 = space of I+J, 2 = space of I+J+L+M, 3 = space of I+Z, 4 = space of A+B+I+J, 5 = space of I+Y+Z. Schultze and Marshall (1993; char. 19), Schultze and Chorn (1997; char. 8), Schultze (2001; char. 19),

Schultze (2004; char. 14).

167. Character 22 of Lloyd *et al*. (2012). J-bone: 0 = present, 1 = space of J+K+L+M, 2 = space of I+J, 3 = space of J+L+M, 4 = space of A+B+I+J, 5 = space of J+C. Schultze and Marshall (1993; char. 22), Schultze and Chorn (1997; char. 2), Schultze (2001; char. 22), Schultze (2004; char. 16).

168. Character 29 of Lloyd *et al*. (2012). Z-bone: 0 = behind skull roof, 1 = integrated into skull roof, 2 = space of Y+Z, 3 = lacking as isolated bone. Schultze and Marshall (1993; char. 29), Schultze and Chorn (1997; char. 12,34), Schultze (2001; char. 29), Schultze (2004; char. 22).

169. Character 30 of Lloyd *et al*. (2012). Lateral line entering skull table through: 0 = bone Z, 1 = bone I, 2 = above bones. Schultze and Marshall (1993; char. 30), Schultze (2001; char. 30), Schultze (2004; char. 23).

170. Character 31 of Lloyd *et al*. (2012). Y-bone: 0 = Y1- and Y2-bones present, 1 = only one Y-bone, 2 = space of X+Y, 3 = space of Y+Z. Schultze and Marshall (1993; char. 31), Schultze and Chorn (1997; char. 13,35), Schultze (2001; char. 31), Schultze (2004; char. 24).

171. Character 32 of Lloyd *et al*. (2012). X-bone: 0 = isolated, 1 = space of X+K, 2 = space of X+Y, 3 = missing. Schultze and Marshall (1993; char. 32), Schultze and Chorn (1997; char. 14), Schultze (2001; char. 32), Schultze (2004; char. 25).

172. Character 34 of Lloyd *et al*. (2012). T-bone: 0 = present, 1 = absent. Schultze and Marshall (1993; char. 34), Schultze (2001; char. 34).

173. Character 36 of Lloyd *et al*. (2012). Bone 10: 0 = present, 1 = absent. Schultze and Marshall

(1993; char. 36), Schultze (2001; char. 36), Schultze (2004; char. 28).

174. Character 37 of Lloyd *et al*. (2012). Bone 11: 0 = present, 1 = absent. Schultze and Marshall (1993; char. 36), Schultze (2001; char. 36), Schultze (2004; char. 28).

175. Character 38 of Lloyd *et al*. (2012). Space taken by L+M: 0 = not present, 1 = present, 2 = space of J+L+M, 3 = space of J+K+L+M (+ possible N), 4 = space of I+J+L+M, 5 = space of K+L+M. Schultze and Marshall (1993; char. 37), Schultze (2001; char. 37), Schultze (2004; char. 29).

176. Character 39 of Lloyd *et al*. (2012). Maxilla and premaxilla: 0 = absent, 1 = present. Schultze and Marshall (1993; char. 38), Schultze (2001; char. 38).

177. Character 57 of Lloyd *et al*. (2012). Ascending process on pterygoid: 0 = absent, 1 = short, 2 = long. Schultze and Marshall (1993; char. 56), Schultze and Chorn (1997; char. 20), Schultze (2001; char. 56), Schultze (2004; char. 40). State ‘2’ only found in post-Palaeozoic Dipnoi.

178. Character 65 of Lloyd *et al*. (2012). Number of infradentaries: 0 = four, 1 = two, 2 = one, 3 = three. Schultze and Marshall (1993; char. 64), Schultze and Chorn (1997; char. 21), Schultze (2001; char. 64), Schultze (2004; char. 43).

179. Character 71 of Lloyd *et al*. (2012). Ossified meckelian bone: 0 = present, 1 = lacking. Schultze and Marshall (1993; char. 70), Schultze (2001; char. 70), Schultze (2004; char. 48).

180. Character 73 of Lloyd *et al*. (2012). Dentition: 0 = dentine plates, 1 = tooth plates, 2 = toothed (shedding denticles). Schultze and Marshall (1993; char. 72), Schultze (2001; char. 72), Schultze (2004; char. 49).

181. Character 74 of Lloyd *et al*. (2012). Form of marginal tooth ridge: 0 = absent, 1 = continuous, 2 = incomplete. Schultze and Marshall (1993; char. 73), Schultze (2001; char. 73).

182. Character 75 of Lloyd *et al*. (2012). Tuberosities on palate: 0 = present and irregular, 1 = arranged radially, 2 = arranged in rows, 3 = absent. Schultze and Marshall (1993; char. 74), Schultze (2001; char. 74).

183. Character 76 of Lloyd *et al*. (2012). 0 = no denticles, 1 = episodically shed denticles. Schultze and Marshall (1993; char. 75), Schultze (2001; char. 75), Schultze (2004; char. 50).

184. Character 77 of Lloyd *et al*. (2012). Tooth plates ridges: 0 = no tooth plates, 1 = without radial pattern, 2 = radial pattern with cusps, 3 = radial pattern without cusps, 4 = parallel ridges. Schultze and Marshall (1993; char. 76), Schultze and Chorn (1997; char. 23,32), Schultze (2001; char. 76).

185. Character 80 of Lloyd *et al*. (2012). Ceratohyal: 0 = short and stout, 1 = long. Schultze and Marshall (1993; char. 79), Schultze and Chorn (1997; char. 26), Schultze (2001; char. 79), Schultze (2004; char. 51).

186. Character 81 of Lloyd *et al*. (2012). Basihyal: 0 = short without denticles, 1 = long and denticulated, 2 = short and denticulated. Schultze and Marshall (1993; char. 80), Schultze (2001; char. 80), Schultze (2004; char. 52).

Notes on characters

Character 5. Pit-lines on B bone: 0. absent; 1. anterior and middle pit-line present; 2. only anterior pit-line; 3. only posterior pit line. *Gnathorhiza* only possesses a posterior pit line which has not traditionally been coded. Here we add this as a fourth state unordered.

Characters amended in the matrix of Kemp *et al.* (2017).

Recoding of *Persephonichthys* is required for Character 21 when considering all lateral line canals. In the supraorbital series and the mandibular bones the lateral line canals are enclosed in bone in *Persephonichthys*.

Uronemus

Character 3 from 1 to 0. *Uronemus* possesses elaborate ornamentation on the surface of the calvarial bones as clearly seen in specimen NMS G 1976.19.3.

Dipterus

Character 3 from 0 to 1. There is no reference to surface ornamention on the calvarial bones of *Dipterus* in White (1965) for instance nor in the many specimens viewed by the authors.

Sagenodus

Character 3 from 0 to 1. There is no reference to surface ornamention on the calvarial bones of *Sagenodus* in the many specimens of the NMS and BMNH viewed by the authors.

Chirodipterus

Character 3 from 0 to 1. There is no reference to surface ornamention on the calvarial bones of *Chirodipterus* in Miles (1977) for instance nor in the specimens viewed by the authors in the BMNH.

Character 7. *Chirodipterus* is polymorphic for this character. An F-bone is present in *Chirodipterus* BMNH P52563 (see Miles, 1977, fig. 118 c).

Ctenodus

Character 2 from 0 to 1. The snout of *Ctenodus* is not mineralised.

Character 3 from 0 to 1. There is no reference to surface ornamention beyond that of the typical radiating ornamentation on the calvarial bones of *Ctenodus*. The ornamentation described in Sharp & Clack (2013) refers to the typical dipnoan radiating pattern and lateral line canal pores.

Conchopoma

Character 9 from 1 to 0. *Conchopoma* possesses a full compliment of periorbital bones as figured by Marshall (1988, figs. 2, 3).

Persephonichthys

Character 14 from 0 to 1. Pardo *et al.* (2014, p.8) clearly state the periorbital bones are incomplete.

Character 65 from 1 to ?. There is no evidence of the structure of the fins in *Persephonichthys.*

Character 68 from 1 to ?

Character 72 from 1 to ?

Character 71 from 1 to ?

Character 70 from 1 to ?

Changes made to matrix of Clack *et al*. (in press).

Ctenodus

Character 2 from ‘?’ to ‘0’. There is no record of a pineal eminence in *Ctenodus*. See review of the genus by Sharp & Clack (2013).

Character 14 from ‘?’ to ‘2’. *Ctenodus* possesses a fused K+L bone. See review of the genus by Sharp & Clack (2013).

Character 16 from ‘0’ to ‘2’. *Ctenodus* possesses a fused K+L bone and so is coded as ‘2’. See review of the genus by Sharp & Clack (2013).

Character 19 from ‘?’ to ‘0’. Sharp & Clack (2013) note the presence of an N-bone in *Ctenodus*.

Character 20 from ‘0’ to ‘1’. A fused Q+N-bone is noted in *Ctenodus* by Westoll (1949).

Character 58 from ‘0’ to ‘1’. Figure 15 in Sharp & Clack (2013) appears to show that the parasphenoid separates the pterygoids for more than half their length but in this specimen the pterygoids are incomplete. Figure 15 shows a more complete specimen where the parasphenoid does note separate the pterygoids for more than half way.

Chirodipterus onawayensis

Character 74 from ‘0’ to ‘1’. *Chirodipterus onawayensis* does not possess coronoid bones. See Schultze (1982).

Characters 93-103 are coded from Ahlberg *et al.* (2006) and have not been recoded here.

Conchopoma

Character 2 from ‘?’ to ‘0’. The pineal eminence is a structure expressed as a slight protrusion on the dermal surface of the skull roof as exemplified by *Diabolepis*, not of the endocast, and as such this character can be coded as ‘0’ for *Conchopoma*.

Character 5 from ‘?’ to ‘0’. Heidtke (1986) and Marshall (1988) demonstrates that neither pit lines nor canals pass through the B-bone of *Conchopoma* and as such it can be coded as ‘0’.

Character 6 from ‘?’ to ‘1’. *Conchopoma* clearly has a single C-bone as figured by Heidtke (1986) and Marshall (1988).

Character 9 from ‘1’ to ‘1, 2’. Whereas Marshall (1988) describes *Conchopoma edesi* as possessing paired E-bones (state ‘1’), Heidtke(1986) demonstrates *Conchopoma gadiforme* as possessing a single bone described as a combined Q-, F-, E-bone. The implication is that the E-bone is present and fused with the Q- and F-bones rather than lost completely and whereas this may be questioned, here we take a pragmatic stance and adopt Heidtke’s (1986) interpretation for *Conchopoma gadiforme*.

Character 13 from ‘?’ to ‘1’. Both Heidtke (1986) and Marshall (1988) interpret and figure the J-bone in *Conchopoma* as being fused with the K- and L-bones and as such it can be regarded as being present and does not meet along the midline.

Character 19. *Conchopoma edesi* does not possess a N-bone whereas *Conchopoma gadiforme* does.

Character 28 from 1 to 0. Marshall (1988) shows that a lateral line is absent in bone 3 in *Concho-poma*.

Character 30 from ‘1’ to ‘2’. *Conchopoma* may not possess a complete circumorbital series. For this character, the only unequivocal coding is for the lack of bones 10 and 11 as these are absent. State ‘0’

may be inapplicable because bones 1 and 2 have not been confidently identified as being present (Marshall, 1988).

Character 31 from ‘2’ to ‘?’. The snout of *Conchopoma* is unossified and so it is not possible to determine this character.

Character 32 from ‘1’ to ‘0’. Bone 6 does reach the ventral margin of the cheek in *Conchopoma*. See Marshall (1988).

Character 33 from ‘0’ to ‘1’. Bone 7 is longer than it is deep in *Gnathorhiza*. See Marshall (1988) fig. 7.

Character 34 from ‘1’ to ‘-’. *Conchopoma* does not possess bone 10 and so this character is coded as being inapplicable.

Character 35 from ‘1’ to ‘?’. The suboperculae are not known in *Conchopoma* and so this character is coded as unknown.

Character 39 from ‘?’ to ‘1’. The lateral margins of the parasphenoid of *Conchopoma edesi* curve ventrally forming an arch shape in transverse section. See Marshall (1988, fig. 8).

Character 40 from ‘?’ to ‘2’. *Conchopoma* possesses a posterior parasphenoid stalk. See Heidtke (1986) and Marshall (1988).

Character 45 from ‘1’ to ‘0’. Dental material is present on the parasphenoid of *Conchopoma*. See Heidtke (1986) and Marshall (1988).

Character 48 from ‘1’ to ‘?’. The otico-occipital is either poorly ossified or not ossified in *Conchopoma* and is not preserved. It is therefore not possible to determine where the parasphenoid lies in relation to the otico-occipital and so this character must be coded as ‘?’.

Character 50 from ‘0’ to ‘?’. To the best of the authors’ knowledge there are no specimens of *Conchopoma* that are preserved in such a way as to be able to determine the state of this character. It is therefore coded as ‘?’.

Character 51 from ‘3’ to ‘2’. The lateral angle of the parasphenoid of *Conchopoma* is rounded rather than reflexed. See Heidtke (1986) and Marshall (1988). A reflexed lateral angle of the parasphenoid is seen in *Neoceratodus.*

Character 52 from ‘?’ to ‘0, 1’. The posterior end of the parasphenoid stalk in *Conchopoma* may terminate in a single point as seen in *Conchopoma gadiforme (*Heidtke , 1986, fig. 3 D) or a single point as in *Conchopoma edesi* (Marshall, 1988, fig. 8).

Character 53 from ‘?’ to ‘1’. The margins of the posterior stalk of the parasphenoid of *Conchopoma* are parallel. See Heidtke (1986) and Marshall (1988).

Character 57 from ‘?’ to ‘1’. *Conchopoma* possesses denticales on the anterolateral margin of the pterygoid. See Marshall (1988).

Character 58 from ‘?’ to ‘0’. The parasphenoid of *Conchopoma gadiforme* separates the pterygoids completely. See Heidtke (1986).

Character 67 from ‘1’ to ‘2’. There is no evidence for an adysmphyseal plate in *Conchopoma*. The structures labelled as ‘da’ in Schultze (1975) and Heidtke (1986 fig. 3) are dentaries whereas those la-

belled as ‘ida’ are considered to be splenials (*cf.* Schultze, 2001*)*.

Character 69 from ‘?’ to ‘1’. The dentary forms a narrow gap with the prearticular in *Conchopoma*. See Heidtke (1986 fig. 3).

Character 70 from ‘?’ to ‘1’. The dentary forms a narrow gap with the prearticular in *Conchopoma*. See Heidtke (1986 fig. 3).

Character 74 from ‘0’ to ‘1’. *Conchopoma* does not possess coronoid bones. See Heidtke (1986) and Marshall (1988).

Character 84 from ‘1’ to ‘?’. The ‘upper lip’ of *Conchopoma* is either poorly cartilagenous or unossified and does not preserve so this character is coded as ‘?’.

Character 85 from ‘?’ to ‘0’. Heidtke (1986) and Marshall (1988) both demonstrate that *Conchopoma* possesses denticles on the dentary and Marshall (1988) provides evidence that the denticles in *Conchopoma* are shed.

Character 86 from ‘?’ to ‘-’. *Conchopoma* does not possess tooth plates and so must be coded as inapplicable for this character.

Character 88 from ‘?’ to ‘-’. *Conchopoma* does not possess tooth plates and the denticles present are neither round nor conical and so this character must be coded as inapplicable.

Character 90 from ‘?’ to ‘-’. *Conchopoma* does not possess large dentine elements that can unequivocally be described as ‘teeth’ - it possesses denticles - and so this character must be coded as inapplicable.

Character 92 from ‘?’ to ‘-’. *Conchopoma* does not possess marginal nlister to the pterygoid/prearticular and so this character must be coded as inapplicable.

Character 104 from ‘0’ to ‘?’. The neurocranium of *Conchopoma* is not preserved so the coding state for this character is unknown.

Character 108 from ‘0’ to ‘?’. The palatoquadrate in *Conchopoma* was cartilagenous or poorly ossified and is not preserved so the coding state for this character is unknown.

Character 141 from ‘?’ to ‘1’. Heidtke (1986) interpret the entopterygoids of *Conchopoma* to overlap the parasphenoid dorsally. We adopt this interpretation for our coding.

Character 144 from ‘?’ to ‘2’. The posterior dorsal fin radials of *Conchopoma* are not supported by basal plates on the neural spines. See Schultze (1975).

Character 145 from ‘?’ to ‘-’. There is no distincct anal fin support in *Conchopoma*. The ventral median fin is a continuous fringe supported by haemal arches and radials. See Schultze (1975).

Character 146 from ‘?’ to ‘1’. The median fin radials in *Conchopoma* are hour-glass shaped. See Schultze (1975).

Character 147 from ‘?’ to ‘0’. The notochord in *Conchopoma* is unrestricted. See Schultze (1975) and Heidtke (1986).

Character 148 from ‘?’ to ‘0’. The neural arches and neural spines are separate in *Conchopoma*. See Schultze (1975) and Heidtke (1986).

Character 157 from ‘?’ to ‘-’. *Conchopoma* does not possess tooth plates and so this character is coded as inapplicable.

Character 159 from ‘0’ to ‘?’. The snout and nasal region and the braincase are not preserved in *Conchopoma* and so this character must be coded as ‘?’.

Gnathorhiza

Character 2 from ‘?’ to ‘0’. The pineal eminence is a structure expressed as a slight protrusion on the dermal surface of the skull roof as exemplified by *Diabolepis*, not of the endocast, and as such this character can be coded as ‘0’ for *Gnathorhiza.*

Character 5 from ‘?’ to ‘3’. *Gnathorhiza* only possesses a posterior pit line which has not traditionally been coded. Here we add this as a fourth state unordered.

Character 6 from ‘?’ to ‘1’. *Gnathorhiza* clearly has paired C-bones as figured by Carlson (1968) and Berman (1976).

Character 13 from ‘?’ to ‘1’. The J-bones of *Gnathorhiza* clearly do not meet in the middle as demonstrated by Carlson (1968) and Berman (1976).

Character 17 from ‘1’ to ‘-’. The X-bone is not present in *Gnathorhiza* and so this character is recoded as being inapplicable.

Character 18 from ‘1’ to ‘0’. Whereas a separate M-bone is not present in the lateral dermal skull series in *Gnathorhiza*, it is interpreted by Carlson (1968) and Berman (1976) to be present and fused with the K- and L-bones and so can be regarded as being present.

Character 22 from ‘?’ to ‘1’. Berman (1976; fig. 1 D) demonstrates that the maximum width of the skull is at the level with, if slightly anterior to, bone Y_1.

Character 28 from ‘1’ to ‘-’. Berman (1976) shows that bone 3 is not present in *Gnathorhiza*. This character is therefore coded as being inapplicable.

Character 29 from ‘1’ to ‘2’. *Gnathorhiza* does not possess a complete circumorbital series. For this character, the only logical coding is for the lack of bones 10 and 11 as these are absent. State ‘0’ is inapplicable because bones 1-3 are also absent (Berman, 1976).

Character 30 from ‘?’ to ‘1’. Berman (1976) illuatrates completely the cheek and orbit region in *Gnathorhiza* which shows that the postorbital cheek is approximately the same length as the orbit and can thus be coded as ‘1’.

Character 31 from ‘1’ to ‘?’. The snout of *Gnathorhiza* is unossified and so it is not possible to determine this character.

Character 32 from ‘?’ to ‘0’. Bone 6 does reach the ventral margin of the cheek in *Gnathorhiza*. See Berman (1976).

Character 33 from ‘?’ to ‘1’. Bone 7 is longer than it is deep in *Gnathorhiza*. See Berman (1976) fig. 1.

Character 34 from ‘?’ to ‘-’. *Gnathorhiza* does not possess bone 10 and so this character is coded as being inappicable.

Character 37 from ‘0’ to ‘1’. The pterygoids of *Gnathorhiza* are separated by the parasphenoid posteriorly but are interpreted to articulate with each other along the antero-lateral margin. See Berman (1976).

Character 40 from ‘?’ to ‘2’. *Gnathorhiza* possesses a posterior parasphenoid stalk. See Carlson (1968) and Berman (1976).

Character 41 from ‘1’ to ‘0’. The parasphenoid of *Gnathorhiza* figured by Berman (1976) shows an unclear distinction between the anterior corpus and the posterior stalk. However, if the stalk is considered to begin either at the thinnest point of the parasphenoid or more anteriorly, the ratio of the posterior portion to the anterior portion is still less than 1 and so this character can be coded as ‘0’.

Character 45 from ‘0’ to ‘1’. Dental material is not present on the parasphenoid of *Gnathorhiza*. See Berman (1976).

Character 48 from ‘1’ to ‘?’. The otico-occipital is either poorly ossified or not ossified in *Gnathorhiza* and is not preserved. It is therefore not possible to determine where the parasphenoid lies in relation to the otico-occipital and so this character must be coded as ‘?’.

Character 50 from ‘0’ to ‘?’. To the best of the authors’ knowledge there are no specimens of *Gnathorhiza* that are preserved in such a way as to be able to determine the state of this character. It is therefore coded as ‘?’.

Character 52 from ‘?’ to ‘3’. The posterior end of the parasphenoid stalk in *Gnathorhiza* is trifid with lateral projections. See Berman (1976) fig. 4 B, J.

Character 53 from ‘?’ to ‘1’. At the narrowest point, the margins of the stalk of the parasphenoid are

subparallel (see Berman, 1976). Towards the posterior the margins actually diverge into the lateral projections.

Character 57 from ‘?’ to ‘2’. *Gnathorhiza* possesses tooth plates anterolateral to the pterygoids. See Berman (1976, fig. 4).

Character 59 from ‘?’ to ‘0’. From Carlson (1968) the angle between midline and anterolateral margin of the pterygoid can be measured as 43° and thus coded as ‘0’.

Character 69 from ‘?’ to ‘-’. The absence of dentary bones in *Gnathorhiza* means that this character must be coded as ‘-’.

Character 70 from ‘?’ to ‘-’. The absence of dentary bones in *Gnathorhiza* means that this character must be coded as ‘-’.

Character 72 from ‘?’ to ‘1’. From the description and figures in Berman (1976, fig. 5) the adductor fossa can measured as being between 5-20% the total jaw length in *Gnathorhiza*.

Charater 74 from ‘?’ to ‘1’. No coronoids are present in *Gnathiorhiza.*

Character 79 from ‘?’ to ‘1’. Specimens figured in Berman (1976, fig. 5) demonstrate that the curvature of the ventral margin is flat in *Gnathorhiza.*

Character 80 from ‘?’ to ‘1’. The glenoid figured in Berman (1976, fig. 7) shows that the glenoid in *Gnathorhiza* is oriented posterodorsally.

Character 82 from ‘?’ to ‘1’. Specimens figured in Berman (1976, fig. 5) demonstrate that the angular

and surangular are fused in *Gnathorhiza.*

Character 83 from ‘?’ to ‘1’. The description and specimens figured in Berman (1976, fig. 5) demonstrate that the splenial and postsplenial are fused in *Gnathorhiza*.

Character 84 from ‘2’ to ‘?’. The ‘upper lip’ of *Gnathorhiza* is either poorly cartilagenous or unossified and does not preserve so this character is coded as ‘?’.

Character 85 from ‘?’ to ‘-’. The absence of dentary bones in *Gnathorhiza* means that this character must be coded as ‘-’.

Character 92 from ‘?’ to ‘-’. *Gnathorhiza* does not possess marginal nlister to the pterygoid/prearticular and so this character must be coded as inapplicable.

Character 108 from ‘0’ to ‘?’. The palatoquadrate in *Gnathorhiza* was cartilagenous or poorly ossified and is not preserved so the coding state for this character is unknown.

Character 141 from ‘?’ to ‘1’. Carlson (1968) and Berman (1976) interpret the entopterygoids of *Gnathorhiza* to overlap the parasphenoid dorsally. We adopt this interpretation for our coding.

Character 159 from ‘0’ to ‘?’. The snout and nasal region and the braincase are not preserved in *Gnathorhiza* and so this character must be coded as ‘?’.

S**upplementary figure 1**. 50% majority rule tree for Bayesian analysis showing nodes with posterior probability <50%.

References

Ahlberg, P. E., Smith, M. M. & Johanson, Z., 2006. Developmental plasticity and disparity in early dipnoan (lungfish) dentitions. *Evolution & development*, **8**(4), 331-349.

Berman, D. S., 1976. Occurrence of *Gnathorhiza* (Osteichthyes: Dipnoi) in aestivation burrows in the Lower Permian of New Mexico with description of a new species. *Journal of Paleontology*, **50**(6), 1034-1039.

Carlson, K. J., 1968. The skull morphology and estivation burrows of the Permian lungfish, *Gnathorhiza serrata*. *The Journal of Geology*, **76**(6), 641-663.

Friedman, M. 2007. The interrelationships of Devonian lungfishes (Sarcopterygii: Dipnoi) as inferred from neurocranial evidence and new data from the genus *Soederberghia* Lehman, 1959. *Zoological Journal of the Linnean Society*, **151**(1), 115-171.

Heidtke, U., 1986. Über Neufunde vonconchopoma gadiforme kner (dipnoi: pisces). *Paläontologische Zeitschrift*, *60*(3-4), pp.299-312.

Kemp, A., 1977. The pattern of tooth plate formation in the Australian lungfish, *Neoceratodus forsteri* Krefft. *Zoological Journal of the Linnean Society*, *60*(3), 223-258.

Kemp, A., Cavin, L. and Guinot, G. 2017. Evolutionary history of lungfishes with a new phylogeny of post-Devonian genera. *Palaeogeography, Palaeoclimatology, Palaeoecology*, **471**, 209-219.

Lloyd, G. T., Wang, S. C. & Brusatte, S. L. 2012. Identifying heterogeneity in rates of morphological evolution: discrete character change in the evolution of lungfish (Sarcopterygii; Dipnoi). *Evolution*, **66**(2), 330-348.

Marshall, C. R. 1988. A large, well preserved specimen of the Middle Pennsylvanian lungfish *Conchopoma edesi* (Osteichthyes: Dipnoi) from Mazon Creek, Illinois, USA. *Journal of Vertebrate Paleontology*, **8**(4), 383-394.

Miles, R. S. 1977. Dipnoan (lungfish) skulls and the relationships of the group: a study based on new species from the Devonian of Australia. *Zoological Journal of the Linnean Society*, **61**(1-3), 1-328.

Pardo, J. D., Huttenlocker, A. K. and Small, B. J. 2014. An exceptionally preserved transitional lungfish from the Lower Permian of Nebraska, USA, and the origin of modern lungfishes. *PloS one*, **9**(9), p.e108542.

Qiao, T. & Zhu, M. 2009. A new tooth-plated lungfish from the Middle Devonian of Yunnan, China, and its phylogenetic relationships. *Acta Zoologica*, **90**(s1), 236-252.

Qiao, T. & Zhu, M. 2015. A new Early Devonian lungfish from Guangxi, China, and its palaeogeographic significance. *Alcheringa: An Australasian Journal of Palaeontology*, **39**(3), 428-437.

Sharp, E. L. and Clack, J. A. 2013. A review of the Carboniferous lungfish genus *Ctenodus* Agassiz, 1838 from the United Kingdom, with new data from an articulated specimen of *Ctenodus* interruptus Barkas, 1869. *Earth and Environmental Science Transactions of the Royal Society of Edinburgh*, **104**(02), 169-204.

Schultze, H. -P., 1975. Die Lungenfisch-Gattung *Conchopoma* (Pisces, Dipnoi). *Senckenbergiana lethaea*, **56**, 191-231.

Schultze, H. -P., 1982. A dipterid dipnoan from the Middle Devonian of Michigan, USA. *Journal of Vertebrate Paleontology*, **2**(2), 155-162.

Schultze, H.-P. 2001. *Melanognathus*, a primitive dipnoan from the Lower Devonian of the Canadian Arctic and the interrelationships of Devonian dipnoans. *Journal of Vertebrate Paleontology*, **21**(4), 781-794.

Schultze, H. -P., 2004. Mesozoic sarcopterygians. *Mesozoic fishes*, *3*, 463-492.

Schultze, H. -P. & Chorn, J. 1997. The Permo-Carboniferous genus *Sagenodus* and the beginning of modern lungfish. *Contributions to Zoology*, **67**(1), 9-70.

Schultze, H. -P. & Marshall, C. R. 1993. Contrasting the use of functional complexes and isolated characters in lungfish evolution. *Memoirs of the Association of Australasian Palaeontologists*, **15**, 211-224.

Thomson, K. S. & Campbell, K. S. W., 1971. The structure and relationships of the primitive Devonian lungfish *Dipnorhynchus sussmilchi* (Etheridge) (Vol. 38). *Peabody Museum of Natural History, Yale University*.

Westoll, T. S. 1949. On the evolution of the Dipnoi. Pp. 112-184 in Jepson, G. L., Mayr, E. & Simpson, G. G. (eds) *Genetics, paleontology and evolution.* Princeton University Press.

White, E. I. 1965. The head of *Dipterus valenciennesi Sedgwick & Murchison. Bulletin of the British Museum (Natural History), Geology*, **11**, 1-45.

#NEXUS
BEGIN DATA;
DIMENSIONS NTAX=76 NCHAR=186;
FORMAT DATATYPE = STANDARD GAP = - MISSING = ? SYMBOLS = " 0 1 2 3 4 5";
MATRIX
Psarolepis
0-0----------0010100?00????00??0????0-000-
0??11000?000?0?2010100000000000000?0?1?0?0??000??0??0?001?00??????0?????0??0?
000000???00??0???????-??-???101????????-??????1?0020010??
Diabolepis
110?002-0?00100------
1001000?00????0000000?10000000000??10001100?0?101000100001 0?0011?00000?11003020
00?0?0?1101?????0?????0??0?01000????10???????????-01-0?0?0???00?00?-
00???01????1???1?
Adololopasmoyasmithae
??0021????111??01????100?111?00???0111011010 1?110110001211 1???011???0????1??????
?0?1?000000?1011??00111??1?00??????????????????????????????????11??????10?0????1??
010?0?00?0101???0????1??11?
Adelargoschultzei
??2011????111??1????0?0?????????????1110211001?21??111????10???01?????????????
??????100000?11?1??0?0??1?????????????????????????????????????0???1??????01?100
??010?11001001???00????1??11?
Amadeodipteruskencampbelli
1002010???1?11??????0?0???
??10??1??0
???21?0(0 2)000?0001??1????1???2??
Andreyevichthysepitomus
1010?12?1111101011??01002111?1??0?0?1102111 01?110011?0122?0???01?????????11?1?1?
?1111000000?11?1??00111??1??0???01???0??
??????????????????????10?03??
Archaeonectespertusus
??????????????????????????????????0??0???
??????????????????????0???0?
??0?10?0?001000???10????1??11?
Asthenorhynchusmeemannae
10110111101110 01?0???100??1110?100??1?11?0?????????1????110????111101????111????
?01?10000010 11?01111?0???12?0???11?11??010?
??0?0?00?0011010000?(1 2)0312??
Barwickiadownunda
1020111110111100100111002111211001111 1?211?01?210111101211 0???010????????111??1?1
1022100000?0??22?10?????1?????????????????????????????????????111110?11?01?1010?0
10001001001111000000000000
Chirodipterusaustralis
1000211?1?11110(0
1)1000110011111011001111011 01?101110100012111121011100011001101111000220 1?03111011
??00110111200020001100001100001 1(0
1)01101100201 0?0?000010001000 1?001000000100110100???11111?
Chirodipterusonawwayensis
??0?????????????????1???0??010??1???011????1??0????????111????????1111????1?????
??1??1??????????0?????0??????0?????????????????????????????????????11??????????00?
00?????0??10??100?01101111110
Chirodipteruswildungensis
1?00??111?11?0?01?????00??0????1???0??0?????????11?????????????????????????????
??????????????????????????01??0?????????????????????????????????????11?????????1001
?0?10?0?00???????00??????????
Chirodipterusliangchengi

??0??????????1????????0011????????1110110??101110100????1112101?????????1????
????1?0?00?0?10?1??0??101112001200000000000?10?0?111?1?1?0?201?????????0010????
??????????????????????????????
Dipnorhynchuscathlesae
0-
?0??1001?0001?????1
?1??1?????0????0?????1???00??1
0??0?????????????????10111101??
Dipnorhynchussussmilchi
0-
0001000?001000000000000000010000?0?02000????00?????00001?0121010000000001100000
10022?1?021010002201 00?1011010200?1??01?000000100000000000200????????0?001-
00?????????????????????????????11111?
Dipnorhynchuskiandrensis
0-
00????000010000000??00??0????0???0??0???
????????????????????????00??0?????????????????????????????????????11??????????00??
00?010?000000??00??????????
Dipnorhynchuskurikae
0-
00??000?00?0?00000??00??000??1???01?0???
??????????????????0?????1??00??0?????????????????????????????????????11?????????-
00??000000000000000100????11111?
Dipterusvalenciennesi
100021(0
1)110111000100001001011111000001101 00?0101101100101?101211111000010011011110002 21
00000?1011??00111111200120000000011101100111111110120111000000100010000000010(0
1)000000001010000000000200
Eoctenodusmicrosoma
????????????????????????????????????12???111?0?2?0?1?????????????????????????????
??1?????????????0
??????????????????????0??10302??
Fleurantiadenticulata
10201110111111111?001111121112110110111?211101121001111111110???0??2???????1111111?11
2?00-
000?0??20?1??????1??0?????????????????????????????????????0112110111?01?10?1001000000
10011110001?203100?
Gogodipteruspaddyensis
??0?????????????????????01?????????0111011 0?00011011000?1?10???0?010001100110?111
100??01?011010?0110011011120002000010000 0?0000?1001101?0???10?????????001?0010?
??0?????????????0000103030?
Griphognathusminutidens
10212110111111101?01001111?111011100120110010012102111101110121 01?20022121110111101
111?1?1?101000001000?1212000211?111100101111?101(0
1)111111211110000101100 1?00?100101000000011??0000020310??
Griphognathussculpta
1?11??101111?1?1?010??11??010??1???0221??????1????2???0?1????????1110????1?????
??0??0?????????????????????1?1??0?????????????????????????????????????10??????????0???
100100000000011000001022310?1
Griphognathuswhitei
1?11??101111?1?1?0?0??11??010??1???0221??101?1?21121??111?????????(1
2)00????1???????0??1?????????????????0?101??0?????????????????????????????????????10
????11???-00?100100000000011010001022310 11
Grossipteruscrassus
???0??????11?????????1???
??0??
????10???00?0??????????10303??

Holodipteruselderae
??(0 1)(0 1)??????11?(0 1)?1????????0??0??????????210??100?(0
1)??0011?????????????????101????1?????????????????????????????????????01??0?????????????
??????????????????????10?????????00??0?010?0?00??01????00?0(1 2)1312?0
Holodipterusgogoensis
101121111?111001??????101?11?01????12011?01001?1???110121?0121011100121101101111
0121?0000101000111110?111200021010010100010 10?111111111201???????11111100100010
?0000??011??00000(1 2)03120?
Howidipterusdonnae
102011111011110010011100211121100111 11?211?01?21011110121 10???010???????111??1?1
1022100000?0??22?10?????1?????????????????????????????????????111110?11?01?1000?0
100(0 1)000100111100?3010302??
Ichnomylaxkurnai
??????????????????????0?????????????????????????????????????0???0??0??0?00011 0?0
00000?1000001010?0?1011???
10?????????????????00(1 2)1011??
Iowadipterushalli
10011101??101111?000100010111100010?????????????????????????????101?0??????????
????2???10?01?00?
0001000?00000110100?0????????
Jarvikiaarctica
1?21012111111011?1?10121??1?11????11?1?1?100??210??11????00????1?????????????????
??1????????2??1????
?0??0?0?00?000???00???10303??
Jesseniaconcentrica
??0101100?0011001 01?100010????????????1100??-
000020?0??0???00???01?????????????????????2?01?010?0??00?0?10????1??1????????????
??????????????????????????????????01??0??0?(1 2)000?00?1111??100????????1?
Melanognathuscanadensis
100??1100????????00???000?????????111?110?0011201100 1???101210101002210011 00??
100121?00000?0??00010?0?1?1?????00?00100?00000??1?????????20?????????????01?00?
10??00??????0????00030213 10??
Nielsenianordica
1?10??21101??4?1??????10??1???
??0??
??0?10?0?01?001???30??????????
Oervigianordica
1?11??211110?1?1?0?0??00??1???
??????????????????????????????0???0???
?0010?0?000011???00????1003??
Orlovichthyslimnatis
1?21?1??211011101???11011?????????????11021??01?0200??10???0012111?200121011101111
11111000000?0??1??00?111?1?0012001???00000101?????????0020?1?????????01 1000?0
??0?0?00??(0 1)1???00???10302??
Palaeodaphusinsignis
??0???000????????
??
?0?????????????????????10?03??
Pentlandiamacroptera
1?2011(1 2)110111(0 1)001010?1(0
1)02??121?0??1110?11??01?11??1000122101210 11??0?????1?11?11?1121100010???????00?
????1??????011??????1?????????????????????111110(0 1)11??1?100?0??0(0
1)0?00??0111100???????2??
Phaneropleuronandersoni
1?00??21(1 2)011?1(0
1)??????0001???1????????2???

??????????????0??111?100?0?1000?00000(
0 1)1??00????????2??
Pillararhynchuslongi
1001?1??00101000100001001010?0????01110100?0101111?000???1112111?000111001101101
111120010010 00?12210?0-
111200121100000001 1001??1?11011?0?20111??????10001?0010001000?00000(0
1)111000100010200
Robinsondipteruslongi
101121101?110001?00?11001????01000?12011?0?001??0??001????012101?110121201101111
101?1?00001010?0001010?1?1200??1010010001010 1??11?1111?11201????????110011???1?
????????????????????0?02131 0?2
Scaumenaciacurta
1020112110111001?000110021112110110(0
1)11021??01?210?1??012210???011??0?????11??11??112?000000?0?11??00110?11????????
?????????????????????????????0122110111?01?1000001000000100110000 01?10302??
Soederberghiagroenlandica
1021211111111111?00111110?1010101 1?1111211100?1102111????1012?01?????????????1?????
?????1?1??????00?00?0???????0?01??101100?11?????0????????21?1?0?111?11001?10?100
1000?0010011011000?2??10??
Sorbitorhynchusdeleaskitus
??02?1????101??01?????00??1????????1110110?01?1111100????11???0??210??1011101111
001???1?1?1110?1??00110111?00?2??????0?001000??1??011??0???1?????????10?01?0??00
?10?0?00??00???000300130000
Speonesydrioniani
0-
0001010?001000000??0001?????????002000???00????????0001?012101000000000110000 1
000?1010001010002101 00?1?1?01??0??0????0???????1??????????20?0???????10001????0
00?000?00?000???0000000100??
Stomiahykusthlaodus
??0??10?0????000001?000????1???????12000???000??????0????1?0???0?????????????
?????0?01?011110?01?0?10?1111010?000?000100000?0?0110000011??1??????????0010 0?0
?0??000??0??00???000??10302??
Tarachomylaxoepiki
??00?1000?101000(0
1)0010000101 1?1?0??0?110???00?????????????10???01?????????????????????1?000000?11
100?0000???1?????????????????????????????????????0???????10?01??00?001000?0000001
01(0 1)00??10302??
Uranolophuswyomingensis
1000011110011000000000000000?00???012010???00?0??0???110100121010010000001100 00
010022?1?1?0?1000001000?101?01??00?1??010?00?????????????201000???01000?1?00?
0001000000?000???000002131 01?
Conchopomagadiforme
1?200?21(1 2)01014?2110111002?1021?01-?1021201100?3?0?2(0
1)1002100???0?112111???1?10?1??11?0-1-1-0-
???000???0???1122-10011??1?11-
0?0101410110221113001120310 02
Delatitiabreviceps
1?20??111?11?0?11??1??002?1?????????????????0?????????????????????????????????
?????2?000???1?100
?0?10?0?000011???00???10302??
Uronemussplendens
1?211111101111??0000111??2?1?????????22?2?11?0?2???1?1?12?????????????????????
????1000000?00123?0???11??1?1010
0120101001011 1??100?1103120?
Gnathorhizaserrata
1?2031212011 3?2-110??002?1021?01-1112?200001?3?0?2310022?0?????1122--
?111?1??11?11?-001000-

1011??0?110??11??????11??1?1110?120221003113
11150111103031?
Megapleuronzangerli
1?20??212010?4?1110???002?1???1????122??11100?41001??????00?????1112????1??1???
????21001??????(1
2)?????1??????0?????????????????????????????????????12?????????1?11?001200010010111
??10011103 02?0
Palaeophichthysparvulus
1?210121211?111011?11??02??0??????11?21???1??1?2???0??112????????1???2????1?????
??????001?????????????1???1???0??011?????????????????????????????122????11????11?0
01201?10010101???0?11103031?
Parasagenodussibiricus
1?10?????11?3?211????0?2?????????122???0000?3???2?????????????????????????????
????2???10?
?0010?2?00??0????0????10303??
Sagenodusinaequalis
1?201121101114111101110 02?11?1100?112202110 0?21001000?2210???011022??1?11?10?1?
?112?101100?1011??00110????0?????????????????????????????2??0122?00?11?01?10?00
120101001013111100111030 20?
Straitoniawaterstoni
1?202121101111121 00??1002?11?1?????????????????????????????????1?????????????
????2?????????????????????????0?????????????????????????????????2?????22?1?011??1?10?
?012011100102 31??00???1??????
Tranodiscastrensis
1?202121101013121001110 02?11?1101?1122??01100?21001010?2?10????11122??0?11?10?0?
?1122001000???????0010???1?0?????????????????????????????2??01??????11?01?10?00
120011001023101000111030 2??
Ctenodus
10202111111112-210010100211 0???00?1112?2(0 1)110(0 1)?2?0(0 1)10(0 1)1(0 1)(0 1)21(0
1)???01(0 1)2????2?211?(0 1)(0 1)?01?112210(0 1)000?10?1??0(0
1)110??1?0?????????1?????????????????????????1122?(0 1)0(0
1)11?01?100???201110001?21??000?01?3040?
Xylognathus
??????????1?????????????????????????????2?1?????????????????????????????????????
???????001100?1???????0???1?????????11?
?????????????????????????????2??
Limanichthys
1?20?1111?111??01????100?????????????????110??2????00?????????????????????????
??11??1?1??
??????0?000000???0??????????
Sinodipterusbeibei
100021111101110?1?00?010???1?????????1?0?????????????????10???0?????????????????
??????000000?11?1??0?110???1???????10?01?????
?????????????????????????2??
Apatorhynchus
102(0 1
2)111111111001?0????1???1???
??1???????
????????????????????????
Erikia
110101000000110000 00?0000000???
??1??0?
?????00?00?000???0??????????
Dipnotuberculus
????????????????????????????????????1?00?????0?????????????????????0100000011000
?0100?2?1?021010002201?0???0????
????????????????????????????????

Cathlorhynchus
1?0?010-
000010000000?1001?01??????????????????????????????????12??1?000000001100000 1????2?
??021010?0?201?0??01??????????
??????????????????????
Harajicadipterus
1001011010101110 10????00???1?0???1??110????????1??????????10????1???0????????????
?????1000000?11?12?0??11??????12?????????????????????????????????????111?01?????
??????????????????????????2??
Xeradipterus
??2111????11?0?1?0101100??11?000???1200110100?1?00100?????0?????10????110?1011?
1?01?100000101 0?02201?10?11??0?????????????????????1?????????????0??00?11?01?????
??????????????????????????1??
Rhinodipterusulrichi
1001211111111101-
0001101101???1???101102111 01?211110?????10???01?00022111110???11???200000??0-
?1???0?10??1?0??2?????????????????????????????????00?0???10??1?00120010000000011
0000000 10302??
Rhinodipteruskimberleyensis
10110?????111??0????11?1?1????1???1120120110112201101????10???0?101???1011101101
111??000000?0-
?11100?1?111?001200?1000010000101111?1?0?00?0110??????101011000?????????????????
??????????2??
Rhinodipterussecans
1?0021101111111??011??0111?????????110?2?1110?2????01????1101??1?000221?11101???
11?22000000?0-
?1??00?1???1?0??2???10?01?000200100??0000???
??00000 10302??
Westollrhynchuslehmanni
0-00?10100001(1 2)?000????0010?????????100?0-
0?010000?00?111?001?111??????????1????????2?????????????????0??????0????????????
??????????????????????????????????0??0??0??000?00?000???000??02000??
Rhynchodipteruselginensis
1?11??211111?1?1?0????110?101?3?????????????????0?????????????????????????????
??????????????????????????1???0?????????????????????????????????????10??????????0?10?
10?10?0?00??0110100???????0??
Eusthenopteron
0-0----------000110-0----1000?0-001000000---
0000000???0000001010---0-00-
00000?0--100-?0???0000-?0-00-10--00-?----------1?00--0?00?
Persephonichthys
10220121211013-00010-101210?21200-111211001011120112111220 0???010122--
101101110 1?11--001010-0-11-
?00111111?0?120001001?1?????011?1?1?????20?1122?1011100 1?1001?1(2
4)022100203011150111103031?
Celsiodon
???0?????????????????????????????????????112121?101?2???101????01?????????????????
??????000??0-????--
???1???1?????????????1?1?0??????0????????????
???1?302??;
END;